LU TP 19-17
June 2019

RENORMALIZATION GROUP EVOLUTION ANALYSIS OF THE GAUGED FROGGATT-NIELSEN MECHANISM IN 2-HIGGS-DOUBLET MODELS

Robin Plantey

Department of Astronomy and Theoretical Physics, Lund University

Master Thesis supervised by Johan Rathsman

(30 credits)

LUND
UNIVERSITY

Abstract

In this thesis, we consider a 2-Higgs-doublet model with a gauged Froggatt-Nielsen mechanism as an extension of the Standard Model. We assume that (i) the theory at the electroweak scale is the low energy limit of a theory defined at a scale Λ_{FN} (ii) the Yukawa couplings at Λ_{FN} are generated by the Froggatt-Nielsen mechanism. The first assumption is enforced by requiring that models be well behaved under Renormalization Group evolution up to Λ_{FN} in two scenarios: $\Lambda_{FN} = 10^5\,\text{GeV}$ and $\Lambda_{FN} = 10^{16}\,\text{GeV}$. We then proceed to find flavon charge assignments that reproduce the correct order of magnitude for fermion masses and quark mixing. The flavon charges are further constrained by anomaly cancellation conditions. Lastly, having identified the parameter space of models consistent with our assumptions and experimental constraints, we evolve these regions up to Λ_{FN} using the RG equations and discuss possible physics at that scale.

Description Scientifique Populaire

Quelles sont les entités élémentaires, indivisibles qui composent notre Univers? Comment interagissent elles pour former tout ce que nous observons dans la nature? Voilà les questions majeures auxquelles la physique des particules tente de répondre. La meilleure réponse à ce jour, "le modèle standard", est une des plus grandes réussites de la physique moderne. Il s'agit d'une théorie qui décrit avec grande précision le comportement de toutes les particules élémentaires connues. Celles-ci interagissent en échangeant d'autres particules, des bosons de jauge, tels que des photons et des gluons. Si on adopte cette vision moderne d'une interaction on pourrait dire, par analogie, que deux personnes qui se passent un ballon ont une interaction répulsive puisque l'émetteur et le receveur reculent. Parmi la quinzaine de particules élémentaires, seules 4 composent la grande majorité de la matière de l'Univers: l'électron, le quark "up", le quark "down" et le neutrino électron. Le modèle standard permet de prédire le résultat des interactions de ces particules et donc d'expliquer la majorité des phenomènes physiques.

Le modèle standard a ses limites, cependant, et notre compréhension reste incomplète. Un des problèmes du modèle standard est la hiérarchie des masses. L'électron, le quark up, le quark down et le neutrino électron existent en 3 générations. Ces 3 générations de particules sont identiques en tout points à l'exception de leur masses. On observe cependant que la $1^{\text{ère}}$ génération est plus légère que la $2^{\text{ème}}$ génération elle même plus légère que la $3^{\text{ème}}$ génération. À ce jour, on ne connait pas la raison pour cette hiérarchie. Il est difficile d'accepter cela comme une simple coïncidence. Dans le modèle standard, la hiérarchie des masses est incluse "à la main", en ajustant 13 de ses 19 paramètres libres de facon à reproduire les observations. Étant donné qu'en physique on cherche à obtenir une compréhension toujours plus fondamentale de la nature, cette situation n'est pas satisfaisante. On considère donc des modèles au-delà du modèle standard pour tenter de progresser.

Dans cette thèse, j'ai étudié une extension du modèle standard qui vise à expliquer la hiérarchie des masses. Pour cela on inclut le mécanisme de Froggatt-Nielsen, une nouvelle interaction qui distingue les particules des 3 générations et permet d'inclure de manière naturelle la hiérarchie des masses dans le modèle standard. J'ai également essayé de prober le comportement de ce modèle aux hautes énergies, c'est à dire quand les particules ont beaucoup d'énergie. Aujourd'hui, les particules les plus énergétiques que l'on observe sont créées au LHC au CERN. Nous n'avons pas la technologie nécessaire pour créer des particules encore plus énergétiques. C'est pourquoi la recherche théorique est importante. Dans ce projet j'ai cherché à découvrir ce que le modèle prédit quand l'énergie des particules est très haute. Pour cela j'ai utilisé un programme pour résoudre un ensemble d'équations. En résolvant ces équations dans différentes situations, on peut connecter les phénoménes observés à différentes énergies. Grâce à ce travail, on pourrait par exemple utiliser les observations réalisées au LHC pour obtenir des indices sur la physique aux très hautes énergies.

Contents

1 Introduction

The Standard Model (SM) of particle physics is arguably one of mankind's greatest intellectual achievements. It describes three of the four known interactions: electromagnetism, the weak interaction and the strong interaction, within a single gauge theory. The SM as we know it is specified by its gauge group $SU(3)_c \otimes SU(2)_L \otimes U(1)_Y$, its particle content and their representation under the gauge group, the symmetry breaking patterns and the value of all the physical parameters in the Lagrangian [1]. The discovery of the Higgs boson in 2012 [2] concluded the search for the SM particles. However when one considers all known elementary particles, there seems to be a pattern: the fermions consist of three generations of a basic set: an up quark, a down quark, a charged lepton and the corresponding neutrino. A fundamental understanding of the existence of three fermion generations is still lacking. This is a major shortcoming of the SM since 13 of the 19 parameters in the SM Lagrangian describe the flavour structure: 6 quark masses, 3 charged lepton masses, 3 quark mixing angles and 1 phase. All of these are free parameters, in the sense that their values are only determined by what we observe. Even worse, the values exhibit a clear hierarchy as shown in Table 1. This hierarchy suggests that there is a flavour structure.

	m_u	m_c	m_t
m_u	1	≈ 480	≈ 13000
m_c		1	≈ 280
m_t			1

	m_d	m_s	m_b
m_d	1	≈ 20	≈ 1000
m_s		1	≈ 50
m_b			1

	m_e	m_μ	m_τ
m_e	1	≈ 200	≈ 3500
m_μ		1	≈ 20
m_τ			1

Table 1: Mass ratios for up quarks (left), down quarks (center) and charged leptons (right) arranged in a matrix $r_{ij} = \frac{m_j}{m_i}$.

There have been attempts to relate the flavour parameters using e.g. grand unification [3] and discrete flavour symmetries [4]. In the Georgi-Glashow Grand Unified Theory (GUT), the $SU(5)$ gauge symmetry forces the down quarks and charged leptons to have the same mass. Of course this relation holds for the running masses at the GUT scale $\sim 10^{16}$ GeV. As the energy scale is lowered the masses split because of the strong interaction which affects the quarks but not the leptons.

In models where a discrete flavour symmetry is imposed, some Yukawa interactions become forbidden. This constrains the form of the Yukawa coupling matrices and thus eliminates some parameters.

A somewhat more modest approach has been proposed by Froggatt and Nielsen [5]. Namely, it may be that the number of flavour parameters cannot be reduced, nevertheless a fundamental theory should explain the hierarchy, i.e. their relative order of magnitude. In the Froggatt-Nielsen mechanism (described in Sect. 3) a broken $U(1)'$ flavour symmetry is used to factor out the order of magnitude of the fermion masses and quark mixing angles, leaving $\mathcal{O}(1)$ free parameters and $U(1)'$ charges. Thus one can eliminate the hierarchy between the flavour parameters by trading masses and mixing angles for $\mathcal{O}(1)$ coefficients and $U(1)'$ charges.

If the $U(1)'$ symmetry is gauged then the charges are severely constrained by anomaly cancellation conditions. As it happens it is difficult to build an anomaly free, realistic model out of the SM and the FN mechanism. The reason is that even when all the SM particles are charged under $U(1)'$, there are not enough $U(1)'$ charges to both reproduce the masses and mixings and at the same time cancel anomalies. However an additional Higgs doublet charged under $U(1)'$ provides sufficient freedom to build realistic, anomaly-free models.

In this thesis, we consider a 2-Higgs-Doublet Model (2HDM) equipped with a gauged Froggatt-Nielsen mechanism as an extension of the SM. These models are relevant as they incorporate the observed flavour physics and inherit the rich phenomenology of 2HDMs. We assume that these models are the low-energy limit of a more fundamental theory defined at the Froggatt-Nielsen scale Λ_{FN}. We investigate the consequences of this assumption using the Renormalization Group (RG) equations. Requiring the models to satisfy stability, tree-level unitarity and perturbativity up to Λ_{FN} we are able to constrain the 2HDM parameter space at the electroweak scale. A priori, we do not know Λ_{FN} so we consider the two representative cases $\Lambda_{FN} = 10^5\,\text{GeV}$ and $\Lambda_{FN} = 10^{16}\,\text{GeV}$. Naturally, we require that the models reproduce the observed fermion masses and quark mixings. In addition we apply experimental constraints from Higgs searches and study their compatibility with the RG evolution requirement. Indeed if these constraints are compatible it would be a hint that nature favours theories that are the low energy limit of a more fundamental theory. Using the RG equations we also investigate the parameters of viable models at Λ_{FN}, thus connecting electroweak physics with the physics at Λ_{FN}.

The structure of this thesis is as follows. In Sect. 2, 3 and 4 the necessary theoretical background is introduced. In Sect. 5 the results of the RGE analysis are presented, Froggatt-Nielsen charge assignments are made and the viable models are explored. Finally, we conclude in Sect. 6.

2 2 Higgs-Doublet Models

In the SM, the scalar sector is minimal in that, after Electroweak Symmetry Breaking (EWSB), the fermions and gauge bosons acquire mass from interactions with a single $SU(2)_L$ Higgs doublet. A larger scalar sector with more than one Higgs doublet is not ruled out however. In a 2HDM one only extends the scalar sector of the SM with an additional Higgs doublet. The gauge group and particle representations are otherwise the same as in the SM. Because of their rich phenomenology and possibility of CP violation, 2HDMs are interesting extensions of the SM and have been studied extensively (see [6] for a review). In this section we describe the theoretical aspects of 2HDMs relevant to this work.

Consider a scalar sector with two Higgs doublets Φ_1 and Φ_2 having hypercharge $Y = \frac{1}{2}$. The most general renormalizable potential is

$$\begin{aligned} V\Big(\Phi_1,\Phi_2\Big) = {} & m_{11}^2\Phi_1^\dagger\Phi_1 + m_{22}^2\Phi_2^\dagger\Phi_2 - \Big[m_{12}^2\Phi_1^\dagger\Phi_2 + h.c\Big] + \frac{1}{2}\lambda_1\Big(\Phi_1^\dagger\Phi_1\Big)^2 \\ & + \frac{1}{2}\lambda_2\Big(\Phi_2^\dagger\Phi_2\Big)^2 + \lambda_3\Big(\Phi_1^\dagger\Phi_1\Big)\Big(\Phi_2^\dagger\Phi_2\Big) + \lambda_4\Big(\Phi_1^\dagger\Phi_2\Big)\Big(\Phi_2^\dagger\Phi_1\Big) \\ & + \left[\frac{1}{2}\lambda_5\Big(\Phi_1^\dagger\Phi_2\Big)^2 + \lambda_6\Big(\Phi_1^\dagger\Phi_1\Big)\Big(\Phi_1^\dagger\Phi_2\Big) + \lambda_7\Big(\Phi_2^\dagger\Phi_2\Big)\Big(\Phi_1^\dagger\Phi_2\Big) + h.c\right]. \end{aligned} \tag{2.1}$$

Since V must be Hermitian, m_{11}^2, m_{22}^2, λ_1, λ_2, λ_3 and λ_4 are real numbers while m_{12}^2, λ_5, λ_6 and λ_7 can be complex. This potential has therefore 14 independent real parameters. In this thesis, we will take all parameters to be real. This reduces the number of parameters to 10 and implies that there is no explicit CP violation coming from the potential.

In a 2HDM there is a possibility for Higgs mediated Flavour Changing Neutral Currents (FCNC). FCNC can be suppressed if each fermion species couples to exactly one Higgs doublet [7]. This is usually done by imposing a $\mathbb{Z}_2$ symmetry on the theory. This is discussed in more detail in Section 2.2. For now let us assume that under $\mathbb{Z}_2$ inversion we have $\Phi_1 \to -\Phi_1$ and $\Phi_2 \to \Phi_2$. The set $\{\Phi_1, \Phi_2\}$, where the Higgs doublets have definite transformation properties under $\mathbb{Z}_2$, is referred to as the generic basis. Notice that the m_{12}^2, λ_6 and λ_7 terms break the $\mathbb{Z}_2$ symmetry. If such a $\mathbb{Z}_2$ symmetry is enforced, the number of parameters needed to specify the potential goes down to 7. Otherwise, we distinguish two types of $\mathbb{Z}_2$ breaking

- Hard breaking: $\lambda_6 \neq 0$ and/or $\lambda_7 \neq 0$
- Soft breaking: $m_{12}^2 \neq 0$ and $\lambda_6 = \lambda_7 = 0$

This distinction is useful in the context of Renormalization Group (RG) evolution. A hard $\mathbb{Z}_2$ breaking, being caused by dimensionless parameters, will start spreading to the Yukawa sector during RG evolution at 2-loop level. On the other hand, a soft $\mathbb{Z}_2$ breaking will not spread since m_{12}^2 has mass dimensions 2 which means it will be suppressed by the renormalization scale in the Yukawa RG equations.

2.1 The Scalar Sector

The vacuum state of a 2HDM should be a minimum of the above potential. As in the SM, there will be symmetry breaking vacua i.e. different from $\langle\Phi_1\rangle = \langle\Phi_2\rangle = 0$. However, because of the additional doublet, the vacuum structure of 2HDMs is richer than that of the SM. In addition to electroweak symmetry-breaking minima, there are CP-breaking and electric charge-breaking minima [8]. In this thesis, we will assume a CP-conserving, electroweak symmetry-breaking vacuum: $\langle\Phi_1\rangle = \frac{1}{\sqrt{2}}\begin{pmatrix}0\\v_1\end{pmatrix}$, $\langle\Phi_2\rangle = \frac{1}{\sqrt{2}}\begin{pmatrix}0\\v_2\end{pmatrix}$, where $v_1^2+v_2^2 \approx (246\,\text{GeV})^2$ is the Higgs Vacuum Expectation Value (VEV). Before discussing the scalar spectrum of the 2HDM let us introduce the concept of doublet bases.

2.1.1 Doublet Bases

Since only the scalar mass eigenstates of Φ_1 and Φ_2 are observed, one has the freedom to perform a $U(2)$ transformation on the Higgs doublets without affecting the scalar physical states [6].

$$H_i = \sum_{j=1,2} U_{ij}\Phi_j \tag{2.2}$$

The Higgs Basis It is convenient to work in a basis where only one of the doublets has a VEV. This basis is called the Higgs basis. In a CP-conserving 2HDM such as the one considered here, the transformation matrix is

$$U = \begin{pmatrix}\frac{v_1}{v} & \frac{v_2}{v}\\ -\frac{v_2}{v} & \frac{v_1}{v}\end{pmatrix} \equiv \begin{pmatrix}\cos\beta & \sin\beta\\ -\sin\beta & \cos\beta\end{pmatrix}. \tag{2.3}$$

Thus the rotation angle between the generic basis and the Higgs basis is determined by the ratio of the VEVs $\frac{v_2}{v_1} = \tan\beta$ and we have

$$\begin{aligned}\langle H_1\rangle &= \cos\beta\langle\Phi_1\rangle + \sin\beta\langle\Phi_2\rangle = \frac{1}{\sqrt{2}}\begin{pmatrix}0\\v\end{pmatrix}\\ \langle H_2\rangle &= -\sin\beta\langle\Phi_1\rangle + \cos\beta\langle\Phi_2\rangle = \begin{pmatrix}0\\0\end{pmatrix}\end{aligned} \tag{2.4}$$

as desired. In this basis we write the potential as

$$\begin{aligned}V\big(H_1,H_2\big) &= Y_1 H_1^\dagger H_1 + Y_2 H_2^\dagger H_2 + \big[Y_3 H_1^\dagger H_2 + h.c\big] + \frac{1}{2}Z_1\big(H_1^\dagger H_1\big)^2\\ &+\frac{1}{2}Z_2\big(H_2^\dagger H_2\big)^2 + Z_3\big(H_1^\dagger H_1\big)\big(H_2^\dagger H_2\big) + Z_4\big(H_1^\dagger H_2\big)\big(H_2^\dagger H_1\big)\\ &+\left[\frac{1}{2}Z_5\big(H_1^\dagger H_2\big)^2 + Z_6\big(H_1^\dagger H_1\big)\big(H_1^\dagger H_2\big) + Z_7\big(H_2^\dagger H_2\big)\big(H_1^\dagger H_2\big) + h.c\right].\end{aligned} \tag{2.5}$$

The transformation of the potential parameters from the generic basis to the Higgs basis can be found in [9].

To study the scalar spectrum one writes H_1, H_2 in terms of excitations about the vacuum state. Two complex doublets contain 8 real degrees of freedom and we write

$$H_1 = \begin{pmatrix} G^+ \\ \frac{1}{\sqrt{2}}(v + \varphi_1 + iG^0) \end{pmatrix} \qquad H_2 = \begin{pmatrix} H^+ \\ \frac{1}{\sqrt{2}}(\varphi_2 + iA^0) \end{pmatrix} \tag{2.6}$$

During EWSB, when $SU(2)_L \otimes U(1)_Y \to U(1)_{\rm EM}$, the three would-be Goldstone bosons are eaten, as in the SM, by the $W^\pm$ and the Z^0 which become massive. The remaining 5 degrees of freedom consist of one charged scalar, two neutral scalars and one neutral pseudo-scalar. The Goldstone modes are easily identified as $G^\pm$ and G^0 since the second doublet, H_2, having no VEV, does not contribute to the EWSB. One can then find the mass squared matrices for the scalars by inserting Eq. (2.6) in Eq. (2.5). For reference, we quote the results from [9]. This means that $H^\pm$ is the physical charged scalar and its mass is given by

$$m^2_{H^\pm} = \frac{1}{2}Y_2 + Z_3 v^2 \tag{2.7}$$

For the neutral scalars, the mass squared matrix is

$$M^2 = \begin{pmatrix} Z_1 v^2 & Z_6 v^2 & 0 \\ Z_6 v^2 & Y_2 + \frac{1}{2}(Z_3 + Z_4 + Z_5)v^2 & 0 \\ 0 & 0 & Y_2 + \frac{1}{2}(Z_3 + Z_4 - Z_5)v^2 \end{pmatrix} \tag{2.8}$$

The bottom right element yields the mass of the pseudoscalar A^0

$$m^2_A = Y_2 + \frac{1}{2}(Z_3 + Z_4 - Z_5)v^2 \tag{2.9}$$

The masses of the scalars[1] can be obtained by diagonalizing the 2×2 block in Eq. (2.8)

$$\begin{aligned} m^2_h &= \frac{1}{2}\left(m^2_A + (Z_1 + Z_5)v^2 - \sqrt{\left[m^2_A + (Z_5 - Z_1)v^2\right]^2 + 4Z_6^2 v^4}\right) \\ m^2_H &= \frac{1}{2}\left(m^2_A + (Z_1 + Z_5)v^2 + \sqrt{\left[m^2_A + (Z_5 - Z_1)v^2\right]^2 + 4Z_6^2 v^4}\right) \end{aligned} \tag{2.10}$$

If one defines α as the angle between the generic basis and the mass basis for the scalars then the rotation angle that diagonalizes Eq. (2.8) is $\beta - \alpha$. That is, the physical scalars H, h are given in terms of the scalars in the Higgs basis φ_1, φ_2 by

$$\begin{pmatrix} H \\ h \end{pmatrix} = \begin{pmatrix} \cos(\beta - \alpha) & \sin(\beta - \alpha) \\ -\sin(\beta - \alpha) & \cos(\beta - \alpha) \end{pmatrix} \begin{pmatrix} \varphi_1 \\ \varphi_2 \end{pmatrix} \tag{2.11}$$

[1] The labels h and H for the neutral scalars are defined by $m_h \leq m_H$.

The Hybrid Basis It appears that 8 parameters are needed to specify a real 2HDM potential that softly breaks the $\mathbb{Z}_2$ symmetry. However one can use the minimization conditions of the potential, the tadpoles equations, to trade two parameters for the VEVs v_1 and v_2. The two VEVs are related by $v_1^2 + v_2^2 \simeq (246\,\text{GeV})^2$ hence one needs only 7 parameters to specify a real 2HDM with a softly broken $\mathbb{Z}_2$ symmetry. The choice of these parameters is arbitrary as long as they are independent.

In the hybrid basis, one trades some potential parameters for physical quantities. The hybrid basis is the set

$$\Big\{ \tan\beta, \cos(\beta-\alpha), m_h, m_H, Z_4, Z_5, Z_7 \Big\} \tag{2.12}$$

This construction was introduced in [9] to make the physical content of a given real 2HDM more apparent. Strictly speaking it is the same doublet basis as the Higgs basis where some parameters have been traded for others. In the hybrid basis the remaining parameters of the Higgs basis are given by [9]

$$\begin{aligned}
Z_1 &= \frac{s^2_{\beta-\alpha} m_h^2 + c^2_{\beta-\alpha} m_H^2}{v^2} \\
Z_6 &= \frac{(m_h^2 - m_H^2) s_{\beta-\alpha} c_{\beta-\alpha}}{v^2} \\
Z_2 &= Z_1 + 2\cot 2\beta (Z_6 + Z_7) \\
Z_3 &= Z_1 + (2\cot 2\beta - \tan 2\beta) \\
Y_1 &= -\frac{1}{2} Z_1 v^2 \\
Y_2 &= Z_1 v^2 - \frac{1}{2}(Z_3 + Z_4 + Z_5) v^2 \\
Y_3 &= -\frac{1}{2} Z_6 v^2
\end{aligned} \tag{2.13}$$

where $s_{\beta-\alpha} \equiv \sin(\beta-\alpha)$ and $c_{\beta-\alpha} \equiv \cos(\beta-\alpha)$.

The hybrid basis provides a good balance between physical clarity and computational efficiency. Indeed having more masses would be inefficient for scans since many configurations would correspond to unrealistic models with very large quartic couplings. We will make use of the hybrid basis when performing scans over the 2HDM parameter space.

2.2 The Yukawa Sector

In a 2HDM, fermions acquire mass via a Higgs Mechanism analogous to the one in the SM. Fermion mass terms arise from Yukawa interaction with the Higgs fields. In the generic basis, the most general Yukawa sector is given by

$$\begin{aligned}
-\mathcal{L}_Y =& \overline{Q}\tilde{\Phi}_1 Y_1^U u_R + \overline{Q}\Phi_1 Y_1^D d_R + \overline{L}\Phi_1 Y_1^L e_R \\
&+ \overline{Q}\tilde{\Phi}_2 Y_2^U u_R + \overline{Q}\Phi_2 Y_2^D d_R + \overline{L}\Phi_2 Y_2^L e_R + h.c.\,,
\end{aligned} \tag{2.14}$$

where $\tilde{\Phi} = i\sigma_2\Phi^*$. Q and L are the left-handed quark and lepton $SU(2)_L$ doublets. u_R, d_R and e_R are the right-handed up quark, down quark and charged lepton $SU(2)_L$ singlets. Lastly, $Y_i^{F=U,D,L}$ are the Yukawa coupling 3×3 matrices of up quarks, down quarks and leptons to Φ_i. We omit the generation index $a = 1, 2, 3$ on all fields and Yukawa couplings. In this study we do not attempt to explain neutrino masses and proceed under the assumption that they are massless.

Since the fermion masses must be preserved under a change of doublet basis, the Yukawa couplings must transform in a way that leaves the Yukawa sector invariant. Requiring invariance of $\Phi_1 Y_1^{F=D,L} + \Phi_2 Y_2^{F=D,L}$ and $\Phi_1^* Y_1^U + \Phi_2^* Y_2^U$ under a change of basis implies the following transformation on the Yukawa couplings

$$\begin{aligned} Y_i'^{D,L} &= \sum_{j=1,2} U_{ij}^* Y_j^{D,L} \\ Y_i'^{U} &= \sum_{j=1,2} U_{ij} Y_j^{U}. \end{aligned} \tag{2.15}$$

Fermion Masses

In the Higgs basis, the Yukawa Lagrangian is

$$\begin{aligned} -\mathcal{L}_Y =& \overline{Q}\tilde{H}_1 \kappa_0^U u_R + \overline{Q} H_1 \kappa_0^D d_R + \overline{L} H_1 \kappa_0^L e_R \\ &+ \overline{Q}\tilde{H}_2 \rho_0^U u_R + \overline{Q} H_2 \rho_0^D d_R + \overline{L} H_2 \rho_0^L e_R + h.c. \end{aligned} \tag{2.16}$$

where κ_0^F and ρ_0^F are the Yukawa couplings in this basis. They can be expressed in terms of Y_1^F and Y_2^F using Eq. (2.15)

$$\begin{aligned} \kappa_0^F &= \cos\beta\, Y_1^F + \sin\beta\, Y_2^F \\ \rho_0^F &= -\sin\beta\, Y_1^F + \cos\beta\, Y_2^F. \end{aligned} \tag{2.17}$$

By construction, in the Higgs basis only H_1 acquires a VEV. Therefore the fermion masses can be obtained by diagonalizing the Yukawa couplings to H_1. Being complex matrices, they can always be made diagonal with positive entries via two independent changes of bases for the right-handed and left-handed fields.

$$\begin{aligned} V_L^U \kappa_0^U V_R^{U\dagger} &= \frac{\sqrt{2}}{v}\mathrm{diag}(m_u, m_c, m_t) \equiv \kappa^U \\ V_L^D \kappa_0^D V_R^{D\dagger} &= \frac{\sqrt{2}}{v}\mathrm{diag}(m_d, m_s, m_b) \equiv \kappa^D \\ V_L^L \kappa_0^L V_R^{L\dagger} &= \frac{\sqrt{2}}{v}\mathrm{diag}(m_e, m_\mu, m_\tau) \equiv \kappa^L. \end{aligned} \tag{2.18}$$

This is an instance of Singular Value Decomposition (SVD) often referred to as a bi-unitary transformation. The interested reader can read more about SVD in Section 6.3 of [10].

As in the SM, one arrives at the CKM matrix

$$V_{\mathrm{CKM}} = V_L^U V_L^{D\dagger} \tag{2.19}$$

by writing the weak charged current in terms of the quark mass eigenstates.

These unitary transformations of the left-handed and right-handed fields bring the Yukawa couplings to H_2 to

$$\begin{aligned} V_L^U \rho_0^U V_R^{U\dagger} &\equiv \rho^U \\ V_L^D \rho_0^D V_R^{D\dagger} &\equiv \rho^D \\ V_L^L \rho_0^L V_R^{L\dagger} &\equiv \rho^L \end{aligned} \tag{2.20}$$

which need not be diagonal. In general, κ_0^F and ρ_0^F will not be simultaneously diagonalizable in this way. However if ρ^F has non-zero off-diagonal elements in the mass eigenbasis then there will be Flavour Changing Neutral Currents (FCNC) mediated by H_2. Experimentally, FCNCs are known to be very suppressed [11] so a reasonable model must reproduce this feature.

2.3 Natural Flavour Conservation with a $\mathbb{Z}_2$ Symmetry

To guarantee that κ_0^F and ρ_0^F are simultaneously diagonalizable it is sufficient that either $Y_1^F = 0$ or $Y_2^F = 0$ [7]. This ensures that $\kappa_0^F \propto \rho_0^F$. Indeed when going to the Higgs basis we have

$$\begin{aligned} \kappa_0^F &= \cos\beta\, Y_1^F \\ \rho_0^F &= -\sin\beta\, Y_1^F \end{aligned} \quad \text{or} \quad \begin{aligned} \kappa_0^F &= \sin\beta\, Y_2^F \\ \rho_0^F &= \cos\beta\, Y_2^F. \end{aligned} \tag{2.21}$$

In other words, if fermion species F couples to exactly one Higgs doublet then there are no FCNCs. This is known as natural flavour conservation since it holds regardless of the parameter values in the Lagrangian. As previously mentioned, natural flavour conservation in a 2HDM can be achieved by imposing a $\mathbb{Z}_2$ symmetry on the theory and having the Higgs doublets transform as

$$\Phi_1 \to -\Phi_1 \quad \text{and} \quad \Phi_2 \to \Phi_2. \tag{2.22}$$

Then letting the right-handed singlets also transform under $\mathbb{Z}_2$ produces the desired effect i.e. that each fermion species couples to exactly one doublet. One possibility, called type II, is to have $u_R \to u_R$, $d_R \to -d_R$ and $e_R \to -e_R$. Then the $\mathbb{Z}_2$ symmetry requires that

$$\begin{gathered} Y_1^U = 0 \quad Y_2^D = 0 \quad Y_2^L = 0 \\ \Longleftrightarrow \\ \rho_0^U = \cot\beta\kappa_0^U \quad \rho_0^D = -\tan\beta\kappa_0^D \quad \rho_0^L = -\tan\beta\kappa_0^L \end{gathered} \tag{2.23}$$

and there are no FCNC mediated by H_2. A 2HDM type is defined by the transformation of the right-handed singlets under $\mathbb{Z}_2$ inversion. Alternatively this can be thought of as assigning a $\mathbb{Z}_2$ charge ± 1 to the right-handed singlets. The 4 distinct types are listed in Table 2. Type I is SM-like in that all fermions couple to the same Higgs doublet. The Yukawa sector of type II is the same as in the Minimal Supersymmetric Standard Model (MSSM). Type X and Y are also referred to as lepton-specific and flipped models. From now on we only consider $\mathbb{Z}_2$-symmetric 2HDMs.

	Type I (SM-like)	Type II (MSSM-like)	Type X (Lepton-specific)	Type Y (Flipped)
Φ_1	$-$	$-$	$-$	$-$
Φ_2	$+$	$+$	$+$	$+$
u_R	$+$	$+$	$+$	$+$
d_R	$+$	$-$	$+$	$-$
e_R	$+$	$-$	$-$	$+$
ρ^U	$\cot\beta\kappa^U$	$\cot\beta\kappa^U$	$\cot\beta\kappa^U$	$\cot\beta\kappa^U$
ρ^D	$\cot\beta\kappa^D$	$-\tan\beta\kappa^D$	$\cot\beta\kappa^D$	$-\tan\beta\kappa^D$
ρ^L	$\cot\beta\kappa^L$	$-\tan\beta\kappa^L$	$-\tan\beta\kappa^L$	$\cot\beta\kappa^L$

Table 2: $\mathbb{Z}_2$ charges for the different 2HDM types.

3 The Froggatt-Nielsen Mechanism

The fermion mass hierarchy implies that the Yukawa couplings span many orders of magnitude. From a theoretical perspective, having free parameters spanning many orders of magnitude is not satisfactory. One would like to have an explanation for at least their order of magnitude. The Froggatt-Nielsen (FN) mechanism is one such attempt [5]. It aims to factor out the order of magnitude of the Yukawas. The remaining couplings are all taken to be of order 1. It may be that these $\mathcal{O}(1)$ couplings are random or cannot be calculated and have to be taken as free parameters. In any case, these free parameters have been stripped from the hierarchy structure.

It remains to explain the hierarchy of the Yukawa couplings. To this end, Froggatt and Nielsen assume a $U(1)'$ global symmetry and a new complex scalar field S with $U(1)'$ or "flavon" charge $+1$. Following the definitions in [12] we let the left-handed fermions doublets have $U(1)'$ charges Q_i, L_i, the charge-conjugated right-handed fermions singlets have charges u_i, d_i and e_i and the Higgs doublets Φ_1 and Φ_2 have charges χ_1 and χ_2. With these definitions the right-handed fermions have charges $-u_i$, $-d_i$ and $-e_i$.

The FN mechanism is the process that generates the Yukawa couplings. In this framework, the order of magnitude of the Yukawa couplings is controlled by interactions with the flavon field S. As an example, Fig. 1 shows the process generating Y^D_{ij}.

$F_{L/R}$ denote the so-called Froggatt-Nielsen fermions. They are additional vector-like fermions with appropriate quantum numbers to ensure flavon charge conservation. We do not investigate these fermions here, we simply assume their existence and that they acquire mass by coupling to a SM singlet scalar field Φ'. Note that, in the FN framework, the $\overline{F_R}\Phi' F_L$ Yukawa couplings are of order $\mathcal{O}(1)$ which implies that $\langle\Phi'\rangle \simeq \Lambda_{FN}$. Let the mass scale of the FN fermions be Λ_{FN} i.e. $m_F \sim \Lambda_{FN}$ for all FN fermions. At low momentum scales compared to Λ_{FN}, when the FN fermion propagators $\frac{1}{\not{p}-m_F}$ can be approximated by $\frac{1}{\Lambda_{FN}}$, the relevant operator for this process is

$$S^{|n^D_{ij}|}\left(\frac{1}{\Lambda_{FN}}\right)^{|n^D_{ij}|}\overline{Q}_i g^D_{ij}\Phi_2 d_{Rj}\,, \tag{3.1}$$

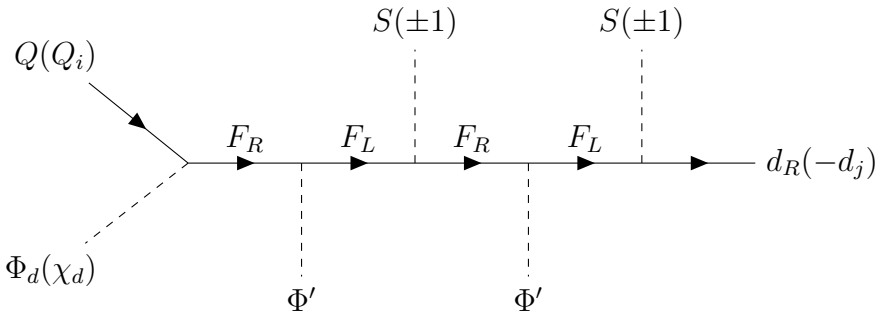

Figure 1: The Froggatt Nielsen mechanism generating $Y^D_{ij} = g^D_{ij}\varepsilon^2$.

where n^D_{ij} is the number of flavon insertions, 2 in the example shown in Fig. 1. The Yukawa couplings to Φ, S and Φ' are taken to be $\mathcal{O}(1)$ so that g^F_{ij}, the product of the former, is also $\mathcal{O}(1)$. Note in passing that this implies that $\langle\Phi'\rangle \sim \Lambda_{FN}$. Now in order for the operator in Eq. 3.1 to be a $U(1)'$ invariant we should have

$$n^D_{ij} = Q_i + d_j - \chi_d \tag{3.2}$$

i.e. conservation of $U(1)'$ charge. One can derive analogously that in general the number of flavon insertions is given in terms of the flavon charges by

$$\begin{aligned} n^U_{ij} &= Q_i + u_j + \chi_u, \\ n^D_{ij} &= Q_i + d_j - \chi_d, \\ n^L_{ij} &= L_i + e_j - \chi_l, \end{aligned} \tag{3.3}$$

where the subscripts $u, d, l = 1$ or 2 depending on the type of $\mathbb{Z}_2$ symmetry. It may happen that $n^F_{ij} < 0$. In this case we must insert S^* which has flavon charge -1 instead of S.

Now if S acquires a VEV $\langle S\rangle$, then the FN operators yield the following Yukawa interactions for the fermions

$$\begin{aligned} &\left(\frac{\langle S\rangle}{\Lambda_{FN}}\right)^{|n^U_{ij}|} \overline{Q}_i g^U_{ij} \tilde{\Phi}_u u_{Rj}, \\ &\left(\frac{\langle S\rangle}{\Lambda_{FN}}\right)^{|n^D_{ij}|} \overline{Q}_i g^D_{ij} \Phi_d d_{Rj}, \\ &\left(\frac{\langle S\rangle}{\Lambda_{FN}}\right)^{|n^L_{ij}|} \overline{L}_i g^L_{ij} \Phi_l e_{Rj}. \end{aligned} \tag{3.4}$$

Letting $\frac{\langle S\rangle}{\Lambda_{FN}} \equiv \varepsilon$, the Froggatt-Nielsen mechanism thus generates Yukawa couplings

$$Y^F_{ij} = g^F_{ij}\varepsilon^{|n^F_{ij}|}, \quad g^F_{ij} \sim \mathcal{O}(1), \tag{3.5}$$

where the order of magnitude has been factored out. Now the order of magnitude of the Yukawa couplings can be adjusted by choosing an appropriate set of flavon charges.

Before proceeding we want to make the statement that $g_{ij}^F \sim \mathcal{O}(1)$ more precise. In order to interpolate Y_{ij}^F between integer powers of ε, we assume that $g_{ij}^F \in [\varepsilon^{\frac{1}{2}}, \varepsilon^{-\frac{1}{2}}]$. This is what we will mean by $\mathcal{O}(1)$ in the remainder of this thesis. Large deviations from $\mathcal{O}(1)$ lead to inconsistencies since the g_i^F are assumed to be stripped of any order of magnitude.

Froggatt and Nielsen have shown that if the Yukawa couplings are ordered, in the sense that $n_{i+1,j}^F \leq n_{i,j}^F$ and $n_{i,j+1}^F \leq n_{i,j}^F$, then to leading order in ε the fermion masses are simply proportional to the diagonal Yukawa couplings

$$m_i^F = \begin{cases} \frac{v_1}{\sqrt{2}} g_i^F \varepsilon^{|n_i^F|}, & F \text{ couples to } \Phi_1 \\ \frac{v_2}{\sqrt{2}} g_i^F \varepsilon^{|n_i^F|}, & F \text{ couples to } \Phi_2 \end{cases}, \tag{3.6}$$

where it is understood that $g_i^F \equiv g_{ii}^F$ and $n_i^F \equiv n_{ii}^F$. Therefore the number of flavon insertions for the diagonal Yukawa interactions is determined by the corresponding mass. This translates into the following constraints for the $U(1)'$ charges

$$\begin{aligned} Q_i - u_i - \chi_u = n_i^U &= \log_\varepsilon \left(\frac{\sqrt{2}}{v_u} m_i^U \right) - \log_\varepsilon(g_i^U), \\ Q_i - d_i + \chi_d = n_i^D &= \log_\varepsilon \left(\frac{\sqrt{2}}{v_d} m_i^D \right) - \log_\varepsilon(g_i^D), \\ L_i - e_i + \chi_l = n_i^L &= \log_\varepsilon \left(\frac{\sqrt{2}}{v_l} m_i^L \right) - \log_\varepsilon(g_i^L), \end{aligned} \tag{3.7}$$

where $\log_\varepsilon() \equiv \frac{\log()}{\log(\varepsilon)}$ is the logarithm in base ε. Of course n_i^F, being a number of flavon (anti-flavon) interactions, must be a positive (negative) integer. This can always be done by a proper choice of $g_{ij}^F \in [\varepsilon^{\frac{1}{2}}, \varepsilon^{-\frac{1}{2}}]$ which corresponds to rounding $\log_\varepsilon \left(\frac{\sqrt{2}}{v_F} m_i^F \right)$ to the nearest integer.

From the ordering of the Yukawa couplings it also follows that the CKM matrix has the following leading order ε-structure (see sect. 4 and 5 in [5])

$$V_{ij}^{CKM} \sim \varepsilon^{|Q_i - Q_j|}. \tag{3.8}$$

The CKM matrix can be expanded in powers of the Cabibbo angle $\sin\theta_C \approx 0.22 \equiv \lambda$ in the Wolfenstein parametrization [13]. At $\mathcal{O}(\lambda^3)$ it has the leading order structure

$$V^{CKM} = \begin{pmatrix} 1 & \lambda & \lambda^3 \\ -\lambda & 1 & \lambda^2 \\ \lambda^3 & -\lambda^2 & 1 \end{pmatrix}. \tag{3.9}$$

This motivates the choice of setting $\varepsilon = \sin\theta_C \approx 0.2$ and imposing the following constraints on the flavon charges

$$\begin{aligned} Q_1 - Q_2 &= 1, \\ Q_2 - Q_3 &= 2. \end{aligned} \tag{3.10}$$

Note that if neutrino masses are included in the model then one has to consider lepton mixing. Reproducing the correct PMNS matrix would then introduce constraints on L_1, L_2, L_3 similar to those of Eq. (3.10).

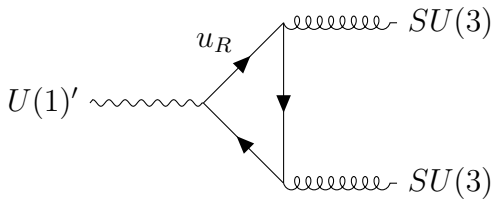

Figure 2: Contribution of the right-handed up quark to the $SU(3)\times SU(3)\times U(1)'$ anomaly. Anomaly cancellation requires that the sum of anomalous contributions from this triangle diagram over all chiral fermions charged under $SU(3)$ and $U(1)'$ vanish.

3.1 The Gauged Froggatt-Nielsen Mechanism

In the original FN mechanism, when the global $U(1)'$ symmetry is broken, one has to live with a pseudo Goldstone boson in the scalar spectrum. These very light bosons are tightly constrained by experiments and in many cases ruled out [11]. Therefore, if our model is to be realistic, the $U(1)'$ symmetry must be gauged. From now on, we only consider such a gauged version of the FN mechanism.

Let us denote the $U(1)'$ gauge boson with Z'. After $U(1)'$ is spontaneously broken by the VEV of the flavon field, the would-be Goldstone boson is eaten by the Z' which acquires a mass $M_{Z'} \approx g'\langle S\rangle = g'\varepsilon\Lambda_{FN}$, where g' is the $U(1)'$ coupling .

3.1.1 Gauge Anomalies

In extending the gauge group of the theory to $SU(3)_c\otimes SU(2)_L\otimes U(1)_Y\otimes U(1)'$, one has to beware of gauge anomalies. These correspond to the failure of a gauge symmetry. Indeed gauge symmetries of the classical theory can be spoiled by quantum effects. In the language of path integrals in quantum field theory, anomalies arise when the integration measure is not invariant under a gauge symmetry of the Lagrangian [14]. Anomaly cancellation can be ensured by requiring that gauge symmetry breaking contributions from the triangle diagrams such as the one in Fig. 2 vanish. A thorough discussion of gauge anomalies is beyond the scope of this work. The interested reader can see e.g. [14] and [15].

In the SM, the gauge anomalies are canceled. When enlarging the SM gauge group with an extra $U(1)$ symmetry one should make sure that possible anomalies involving $U(1)'$ are canceled. Only chiral fermions i.e. fermions for which a mass term is prohibited by the symmetries of the theory, contribute to anomalies [15]. Thus all the SM fermions contribute to the anomalies but not the FN fermions. Indeed we assumed that the FN fermions $F_{L/R}$ are vector-like i.e. their right-handed and left-handed components are in the same representation of the gauge group and therefore mass terms like $\overline{F_L}F_R$ are gauge invariant.

In this work, we do not attempt to include neutrino masses, therefore we will take neutrinos to be uncharged under $U(1)'$. This implies that neutrinos do not contribute to the anomalies.

The anomaly cancellation conditions for a $U(1)'$ extension of the SM are [15]

$$\begin{aligned}
\mathcal{A}_{11'1'} &= 2\sum_i^3 \left(Q_i^2 - 2u_i^2 + d_i^2 - L_i^2 + e_i^2\right) = 0, \\
\mathcal{A}_{111'} &= \frac{2}{3}\sum_i^3 \left(Q_i + 8u_i + 2d_i + 3L_i + 6e_i\right) = 0, \\
\mathcal{A}_{331'} &= \frac{1}{2}\sum_i^3 \left(2Q_i + u_i + d_i\right) = 0, \\
\mathcal{A}_{221'} &= \frac{1}{2}\sum_i^3 \left(3Q_i + L_i\right) = 0, \\
\mathcal{A}_{1'1'1'} &= \sum_i^3 \left(6Q_i^3 + 3u_i^3 + 3d_i^3 + 2L_i^3 + e_i^3\right) = 0, \\
\mathcal{A}_{gg1'} &= 2\sum_i^3 \left(6Q_i + 3u_i + 3d_i + 2L_i + e_i\right) = 0,
\end{aligned} \tag{3.11}$$

where the indices refer to the gauge symmetries involved in the anomaly and g stands for gravity. For example $\mathcal{A}_{gg1'}$ is the gravity $\times$ gravity $\times$ $U(1)'$ anomaly.

The mass constraints Eq. (3.7), CKM constraints Eq. (3.10) and anomaly cancellations Eq. (3.11) define a system of polynomial equations for the $U(1)'$ charges. We will not require that $\mathcal{A}_{1'1'1'}$ and $\mathcal{A}_{gg1'}$ vanish. These anomalies only involve gauge bosons that have not been observed, hence they could be canceled by unknown, non-SM particles. The remaining equations are all linear except for $\mathcal{A}_{11'1'} = 0$ which is quadratic. Thus one cannot in general solve this system of equations using linear algebra. We will instead use methods from algebraic geometry implemented in `Sage`[16] to find solutions.

Gröbner bases The first step in finding the solutions of a system of equations is often to transform it to a simpler form i.e. to a set of simpler equations with the same solutions. For linear equations this is done by putting the system in triangular form using e.g. Gaussian elimination. There exists a generalization to systems of polynomial equations and the simpler set of equations is called a Gröbner basis. The precise definitions of the mathematical objects involved in defining Gröbner bases are irrelevant to this work but the mathematically inclined reader can see e.g. [17]. It suffices to know that the Hilbert basis theorem guarantees that every set of polynomials has a finite Gröbner basis. The precise statement and proof of this theorem can be found in [17].

We will simply give an intuitive understanding of the concept of Gröbner bases. Let $E = \left\{p_i \in \mathbb{Q}[x_1, x_2, ..., x_n]\right\}_{i=1...k}$ be a set of k polynomials in n variables with coefficients in $\mathbb{Q}$[2]. Suppose we have another set of polynomials $G = \left\{g_l \in \mathbb{Q}[x_1, x_2, ..., x_n]\right\}_{l=1...d}$ such

[2]In this work we will only encounter polynomials with rational coefficients. However this argument is not specific to $\mathbb{Q}$ and holds for any field $\mathbb{F}$.

that

$$p_i = \sum_{l=1}^{d} q_l^{(i)} g_l \,, \quad i = 1...n, \tag{3.12}$$

with $q_l^{(i)} \in \mathbb{Q}[x_1, x_2, ..., x_n]$. Then solving the system $p_i = 0$ is equivalent to solving the system $g_l = 0$. A Gröbner basis is such a set. In addition, Gröbner bases have the desirable property that they eliminate variables. To illustrate this, consider the following example from [17]. Suppose we wish to solve the system

$$\begin{cases} p_1(x,y,z) = x^2 + y + z - 1 = 0 \\ p_2(x,y,z) = x + y^2 + z - 1 = 0 \\ p_3(x,y,z) = x + y + z^2 - 1 = 0 \end{cases} . \tag{3.13}$$

A Gröbner basis for these polynomials is the set

$$\begin{aligned} g_1 &= x + y + z^2 - 1, \\ g_2 &= y^2 - y - z^2 + z, \\ g_3 &= 2yz^2 + z^4 - z^2, \\ g_4 &= z^6 - 4z^4 + 4z^3 - z^2. \end{aligned} \tag{3.14}$$

One can check that p_1, p_2, p_3 can be written in terms of g_1, g_2, g_3, g_4 as in Eq. (3.13). This generalizes the triangular form of a linear system of equations. While there are more equations, they are simpler in that g_4 only involves z and g_2, g_3 only involve y and z. One can thus solve $g_4 = 0$ using conventional one variable methods and proceed by backward substitution to find the possible values of y and then x. That Gröbner bases eliminate variables one by one, yielding at least one single variable equation, is general and is guaranteed by the elimination theorem (See Sect. 3.1 in [17]).

When applying these methods to finding anomaly free sets of charges, rational solutions are of particular interest. However such solutions need not exist. For an arbitrary system of equations, showing the existence of rational solutions is highly non-trivial. In this work however, it turns out that the systems of equations considered have a Gröbner basis comprising only of linear equations with rational coefficients. Hence we will only encounter rational charges.

4 Renormalization Group Equations

In quantum field theory, observables such as cross sections and decay widths are typically calculated using perturbation theory. When considering all the processes that contribute to an observable, one encounters processes involving loops. These truly quantum effects often correspond to divergent terms in the perturbation series. This is because fluctuations of arbitrarily high energy are allowed. Yet physical observables are finite. Renormalization reconciles these two apparently irreconcilable facts. The idea of renormalization is that the bare parameters in the Lagrangian are not physical since we only measure the result of the perturbation series. Thus one can redefine the parameters of the theory so as to cancel divergences in the physical observables.

4.1 Renormalization of λ in ϕ^4-theory

To illustrate the renormalization procedure we consider ϕ^4-theory. We will show how the quartic coupling λ is renormalized at 1-loop order and how this leads to the differential equation governing the dependence of λ on the energy scale, the Renormalization Group (RG) equation.

We start by writing the Lagrangian of ϕ^4-theory in terms of the bare parameters m_0 and λ_0 and the bare field ϕ_0.

$$\mathcal{L} = \frac{1}{2}\partial^\mu\phi_0\partial_\mu\phi_0 - \frac{1}{2}m_0^2\phi_0^2 - \frac{\lambda_0}{4!}\phi_0^4. \tag{4.1}$$

Now, in so-called renormalized perturbation theory one writes the bare parameters in terms of the physical coupling, mass, field and their counter-terms as

$$\begin{aligned} \lambda_0 &= (1+\delta_\lambda)\lambda \equiv \lambda Z_\lambda, \\ m_0 &= (1+\delta_m)m \equiv mZ_m, \\ \phi_0 &= Z^{\frac{1}{2}}\phi, \end{aligned} \tag{4.2}$$

where the counter-terms $\delta_\lambda = \mathcal{O}(\lambda^2)$ and $\delta_m = \mathcal{O}(m^2)$ and the physical parameters are defined by a physical measurement. For example one can define a physical quartic coupling by the scattering amplitude measured at some energy scale.

With these definitions the Lagrangian now reads

$$\mathcal{L} = \frac{1}{2}Z\partial^\mu\phi\partial_\mu\phi - \frac{1}{2}m^2Z_mZ\phi^2 - \frac{\lambda}{4!}Z^2\phi^4 - \frac{\delta_\lambda}{4!}Z^2\phi^4. \tag{4.3}$$

The point is that one can now compute observables to a given order in λ and adjust the counter-terms to cancel the divergences at that order [18]. This is perfectly allowed since it corresponds to a redefinition of the bare parameters.

To illustrate, let us calculate the scattering amplitude for $\phi\phi \to \phi\phi$ in renormalized perturbation theory. At order $\mathcal{O}(\lambda^2)$, the following diagrams contribute to the scattering

amplitude

$i\mathcal{M} =$ 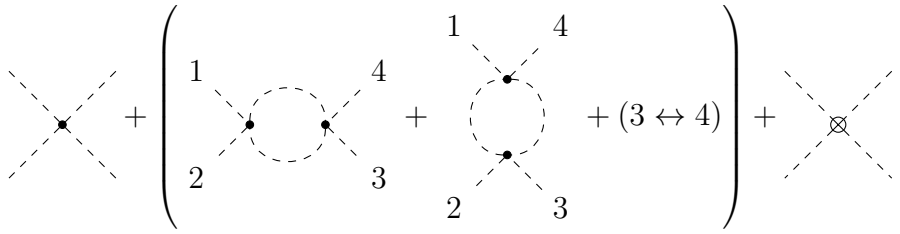

$$= -i\lambda + i\mathcal{M}^{(\text{1-loop})} - i\delta_\lambda. \tag{4.4}$$

Using the Feynman rules it can be seen that the contribution from the 1-loop diagrams $\mathcal{M}^{(\text{1-loop})} \sim \int \frac{d^4k}{k^4}$ has a logarithmic divergence. We calculate $\mathcal{M}^{(\text{1-loop})}$ in dimensional regularization in Appendix A and find

$$i\mathcal{M}^{(\text{1-loop})} = i\frac{3\lambda^2}{16\pi^2}\left(\frac{1}{\varepsilon} + \ln\frac{\mu}{m}\right), \tag{4.5}$$

where μ is an energy scale which has been inserted to keep $\mathcal{M}^{(\text{1-loop})}$ dimensionless during dimensional regularization. Now the divergent term in this expression can be canceled by choosing the counter-term

$$\delta_\lambda = \frac{3\lambda^2}{16\pi^2}\frac{1}{\varepsilon} \tag{4.6}$$

and one arrives at a finite result for the scattering amplitude

$$i\mathcal{M} = -i\lambda + i\frac{3\lambda^2}{16\pi^2}\ln\frac{\mu}{m}. \tag{4.7}$$

Notice that $\mathcal{M}$ now appears to depend on μ, an arbitrary energy scale introduced during regularization. However physical observables cannot depend on the details of the calculation hence we must require that

$$\begin{gathered} \mu\frac{d}{d\mu}\mathcal{M} = 0 \\ \Longleftrightarrow \\ \mu\frac{\partial}{\partial\mu}\lambda \equiv \beta_\lambda = \frac{3\lambda^2}{16\pi^2} + \mathcal{O}(\lambda^3), \end{gathered} \tag{4.8}$$

which implies that the physical coupling must depend on μ. This dependence is contained in the function β_λ which can be solved for recursively with Eq. (4.8). Therefore, to order $\mathcal{O}(\lambda^2)$ one has

$$\beta_\lambda = \mu\frac{\partial}{\partial\mu}\lambda = \frac{3\lambda^2}{16\pi^2}. \tag{4.9}$$

This is the 1-loop RG equation for the quartic coupling in ϕ^4-theory, it encodes the dependence of the physical coupling on the energy scale.

4.2 2HDM Renormalization Group Equations

In principle one can proceed as described in the preceding section, renormalize all the parameters of a 2HDM at a given loop order and find the RG equation for each parameter. For a general 2HDM the RG equations is a set of 129 coupled ordinary differential equations [19]. At 2-loop, these equations are quite long and it would not be particularly enlightening to display them here. We instead refer to the `2HDME` code [20] where the 2-loop RG equations can be found.

Now, each point in the 2HDM parameter space corresponds to a model with given values for all its parameters. As the energy scale changes, each model has a trajectory in parameter space governed by the RG equations. As is well known, the trajectory is only determined once a set of boundary conditions has been specified. A natural choice is for example to fix the values of the parameters at some energy scale.

4.2.1 Constraints

At any given energy scale the 2HDM must be a well behaved quantum field theory. By well behaved we mean that the following constraints should be satisfied in the scalar sector: stability of the vacuum, tree-level unitarity of the S-matrix and perturbativity.

Stability The vacuum of the theory should be a stable minimum of the potential. This means that the potential cannot tend to $-\infty$ in any field direction [21]. Because of gauge invariance the potential can only depend on $\Phi_1^\dagger\Phi_1$, $\Phi_2^\dagger\Phi_2$, $\Phi_1^\dagger\Phi_2$ and $\Phi_2^\dagger\Phi_1$. One can parametrize these terms as

$$\Phi_1^\dagger\Phi_1 = r\cos\gamma, \qquad \Phi_2^\dagger\Phi_2 = r\sin\gamma, \qquad \Phi_1^\dagger\Phi_2 = (\Phi_2^\dagger\Phi_1)^* = \rho e^{i\theta}, \tag{4.10}$$

with $r \in [0, +\infty)$, $\gamma \in [0, 2\pi]$, $\rho \in [0, 1]$ and $\theta \in [0, 2\pi]$. Rewriting the quartic part of the potential in Eq. (2.1) with $\lambda_6 = \lambda_7 = 0$ and requiring that it be positive for all γ, ρ, θ, one finds constraints on the quartic couplings. For a 2HDM potential with all real parameters and no hard $\mathbb{Z}_2$ breaking (i.e. $\lambda_6 = \lambda_7 = 0$) the following conditions are necessary and sufficient for stability [21]

$$\lambda_1, \lambda_2 > 0, \qquad \lambda_3 + \min(0, \lambda_4 - |\lambda_5|) > -\sqrt{\lambda_1\lambda_2}. \tag{4.11}$$

Tree-level Unitarity For a weakly coupled theory, the tree level S-matrix should be close to unitarity because the higher order corrections are small. This requirement can be implemented by considering either the eigen values [22] or the partial wave expansion [23] of the tree level S-matrix. This leads to additional constraints on the quartic couplings.

Perturbativity One would like to keep the theory weakly coupled and allow observables to be calculated using perturbative expansions in the couplings. In a 2HDM this means that all the quartic couplings should be small. Note that even if one is not interested in performing perturbative calculations with some of the quartic couplings these couplings

would still need to be small. Indeed, the RG equations form a set of coupled differential equations, so if one coupling becomes large, it will accelerate the growth of the others. It is customary to use the following perturbativity limit

$$|\lambda_i| < 4\pi. \tag{4.12}$$

The purpose of imposing this weak condition on the quartic couplings is to signal a Landau pole. Indeed when this limit is violated, it usually means that one or more couplings are diverging.

We define the breakdown scale of a model as the largest scale where tree-level unitarity, stability and perturbativity are satisfied.

5 Results

5.1 2HDM Parameter Space Scans

In order to investigate the influence of the 2HDM parameters on the RG evolution of the models we solve the 2-loop RG equations using the `C++` program `2HDME` [20]. As a boundary condition we specify the models at the top (pole) mass scale $m_t = 173\,\text{GeV}$ with the SM gauge couplings and fermion masses in the $\overline{\text{MS}}$ scheme taken from [24] and [25]

$$\begin{aligned}
g_1(m_t) &= 0.35830 & g_2(m_t) &= 0.64779 & g_3(m_t) &= 1.1666 \\
\overline{m}_u(m_t) &= 0.00122\,\text{GeV} & \overline{m}_c(m_t) &= 0.590\,\text{GeV} & \overline{m}_t(m_t) &= 162.9\,\text{GeV} \\
\overline{m}_d(m_t) &= 0.00276\,\text{GeV} & \overline{m}_s(m_t) &= 0.052\,\text{GeV} & \overline{m}_b(m_t) &= 2.75\,\text{GeV} \\
\overline{m}_e(m_t) &= 0.000485\,\text{GeV} & \overline{m}_\mu(m_t) &= 0.102\,\text{GeV} & \overline{m}_\tau(m_t) &= 1.74215\,\text{GeV}
\end{aligned}$$

where g_1, g_2 and g_3 are the couplings for $U(1)_Y$, $SU(2)_L$ and $SU(3)_c$, respectively.

In the scalar sector we scan over boundary conditions for the 2HDM potential at m_t in a large region of parameter space. As already argued above the scans are done in the Hybrid basis

$$\{\cos(\beta-\alpha),\, \tan\beta,\, m_h,\, m_H,\, Z_4,\, Z_5,\, Z_7\}$$

as it provides a handle on physically relevant parameters (e.g. m_H). We restrict our attention to models where the observed 125 GeV Higgs boson is h, the lighter one. Therefore we always set $m_h = 125\,\text{GeV}$ and let $m_H \in \left[125, 900\right]\,\text{GeV}$. The quartic couplings Z_4, Z_5 and Z_7 are allowed to vary in $\left[-\frac{\pi}{2}, +\frac{\pi}{2}\right]$. This is a natural choice since the perturbativity limit is set to $|4\pi|$ and a high perturbativity breakdown requires small quartic couplings. We study the influence of $\tan\beta = \frac{v_2}{v_1}$ on the running by considering three representative values $\{1.1, 5, 25\}$. This region of parameter space was scanned uniformly and $\mathcal{O}(10^5)$ points were found for each type of 2HDM. For a given parameter point, `2HDME` solves the 2-loop RG equations for the corresponding 2HDM and the breakdown scale is calculated. Since the highest energy scale considered in this work is the GUT scale $\sim 10^{16}\,\text{GeV}$, the RG evolution is stopped when either the scale $10^{16}\,\text{GeV}$ is attained or the breakdown scale is reached.

Using these scans, we would like to identify parameter space regions that are well behaved under RG evolution.

5.1.1 Softly Broken $\mathbb{Z}_2$ Symmetry

We first look at the RG evolution of a 2HDM with a softly broken $\mathbb{Z}_2$ symmetry. Fig. 3, 4 and 5 show how the 2HDM parameters affect the breakdown scale for models with $\tan\beta = 1.1$, 5 and 25. On these figures, only the combinations of parameters exhibiting significant correlations are shown.

First of all we find that the type of $\mathbb{Z}_2$ symmetry doesn't affect the correlations. This is expected since the coupling between the Yukawa sector and the scalar sector is a 2-loop

effect. Note that the data shown here is for a type II model but other types exhibit very similar correlations.

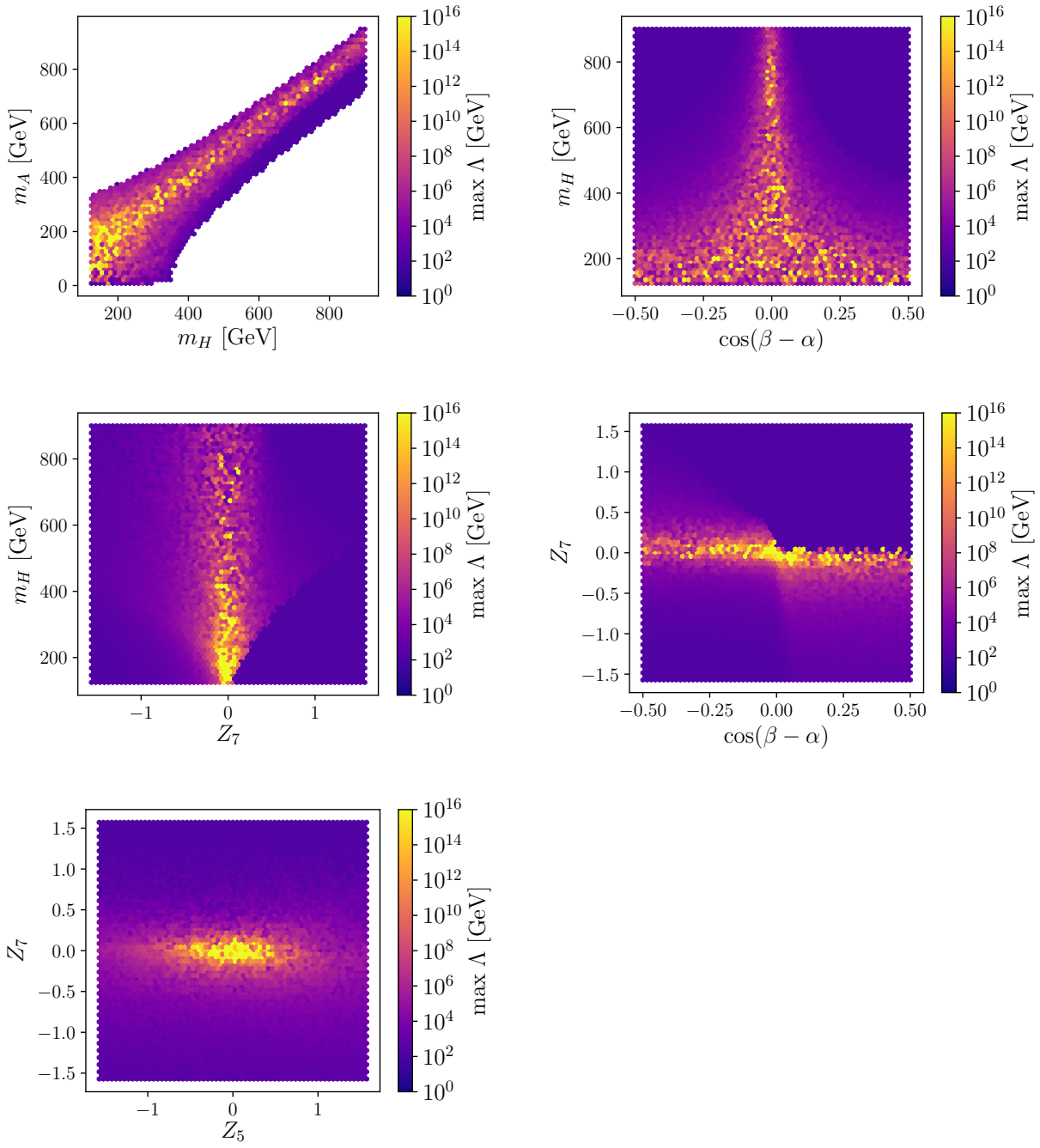

Figure 3: The breakdown scale as a function of 2HDM parameters for the case of a softly broken $\mathbb{Z}_2$ symmetry and $\tan\beta = 1.1$. In each bin the maximum breakdown scale obtained is plotted.

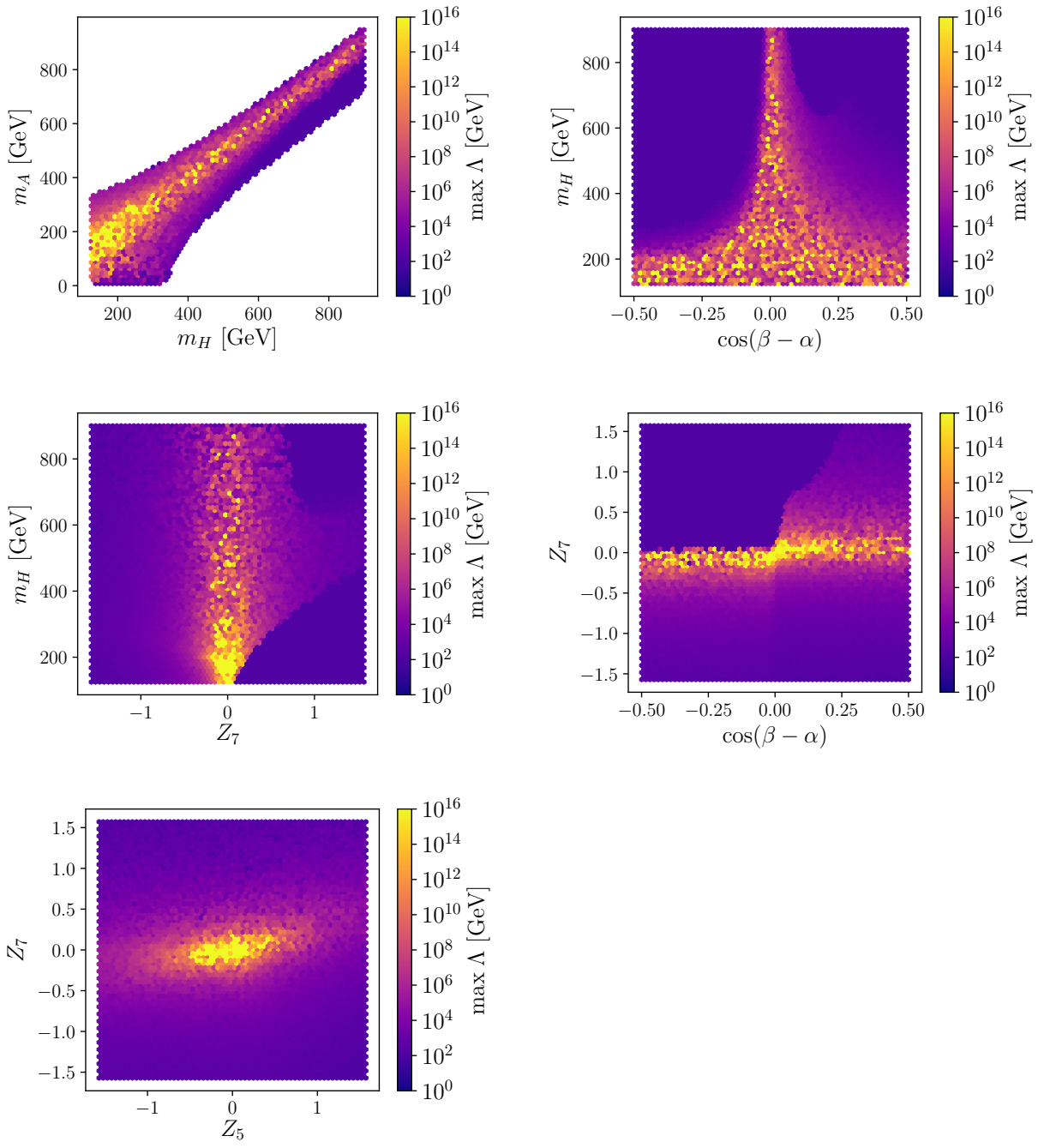

Figure 4: The breakdown scale as a function of 2HDM parameters for the case of a softly broken $\mathbb{Z}_2$ symmetry and $\tan\beta = 5$. In each bin the maximum breakdown scale obtained is plotted.

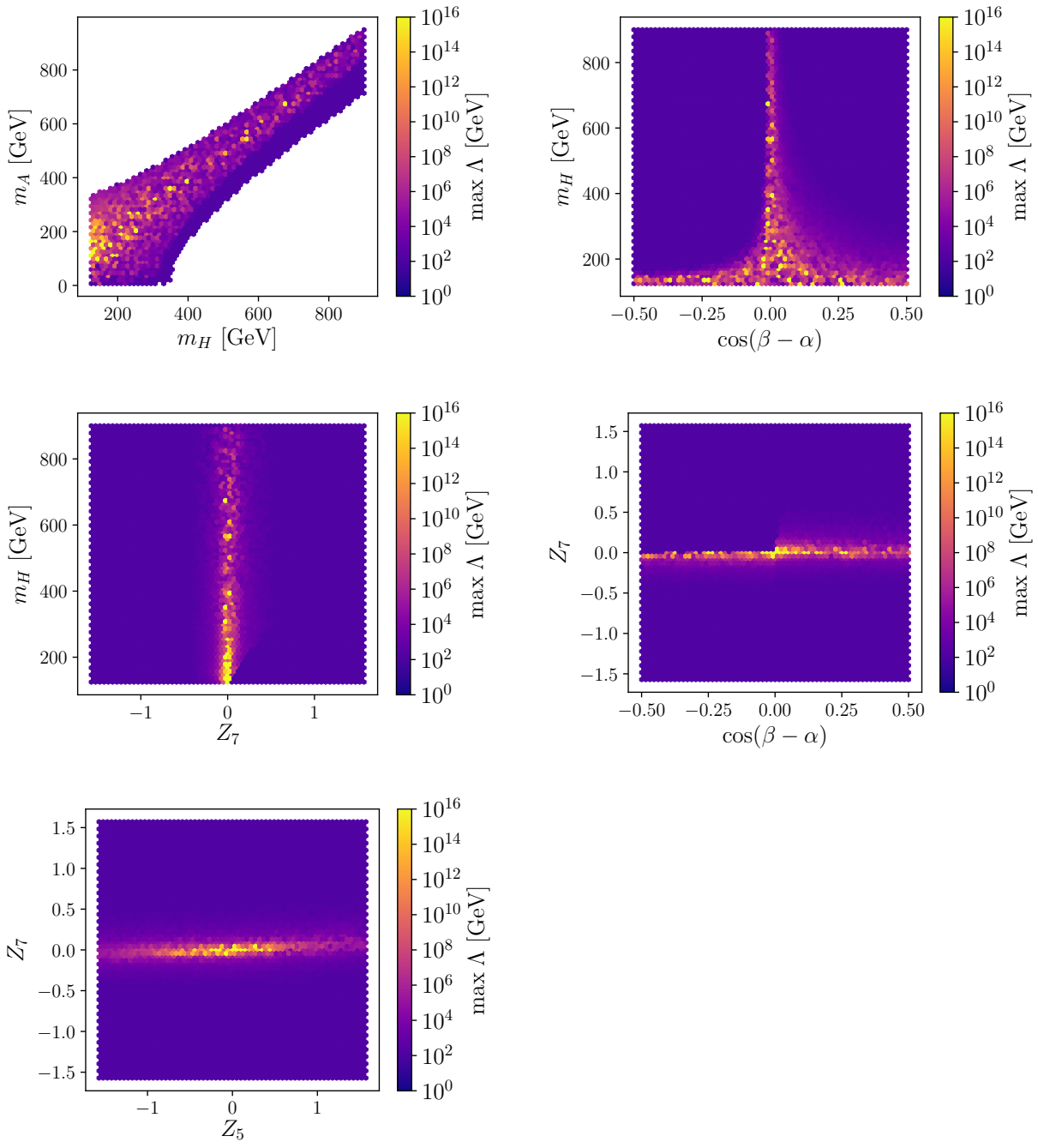

Figure 5: The breakdown scale as a function of 2HDM parameters for the case of a softly broken $\mathbb{Z}_2$ symmetry and $\tan\beta = 25$. In each bin the maximum breakdown scale obtained is plotted.

It can be seen that a heavy H boson requires $c_{\beta-\alpha}$ to be small. On the other hand, for a light H boson, $c_{\beta-\alpha}$ can be as large as 0.5. However, since the coupling of H to vector bosons is proportional to $c^2_{\beta-\alpha}$ [26], if this parameter becomes too large and m_H is low, then H would have been observed in experiments. We find that such models are excluded by experimental constraints in Sect. 5.4.2 .

We note the critical role of Z_7 in determining the breakdown scale compared to the other quartic couplings Z_4 and Z_5. For $\tan\beta = 1.1$, it was found that while a breakdown scale of at least 10^{16} GeV requires $|Z_7| \lesssim 0.25$ one can have $|Z_{4,5}| \lesssim 0.5$. It was shown in [19] that the quartic couplings in the generic basis must be small to attain high breakdown scales. We can relate $|Z_7|$ to the sum of the quartic couplings in the generic basis $\sum_i |\lambda_i|$ using the relation from [9]

$$\begin{aligned} Z_7 = -\frac{1}{2}\sin^2\beta \sin 2\beta\lambda_1 + \frac{1}{2}\cos^2\beta \sin 2\beta\lambda_2 + \frac{1}{2}\cos 2\beta \sin 2\beta\lambda_3 \\ + \frac{1}{2}\cos 2\beta \sin 2\beta\lambda_4 + \frac{1}{2}\cos 2\beta \sin 2\beta\lambda_5, \end{aligned} \tag{5.1}$$

where we have used that $\lambda_6 = \lambda_7 = 0$ for a softly broken $\mathbb{Z}_2$ symmetry. From the above equation we have an inequality valid for all 2HDM with an exact $\mathbb{Z}_2$ symmetry

$$\sum_{i=1} |\lambda_i| > 2|Z_7|. \tag{5.2}$$

Hence a large Z_7 causes an early perturbativity breakdown.

We also observe that a high breakdown scale forces the mass of the pseudo scalar A^0 to be close to that of H. This can be understood from the correlations discussed above and the theoretical relation between m_H and m_A

$$m_A^2 = m_H^2 s^2_{\beta-\alpha} + m_h^2 c^2_{\beta-\alpha} - Z_5 v^2. \tag{5.3}$$

If $m_H \simeq m_h$, then $m_A^2 \simeq m_H^2 - Z_5 v^2$. On the other hand if m_H is large then $\cos(\beta-\alpha)$ must be small hence also $m_A^2 \simeq m_H^2 - Z_5 v^2$. Therefore for models that can be evolved up to high scales there is the relation

$$m_A^2 \simeq m_H^2 - Z_5 v^2. \tag{5.4}$$

The mass of the charged Higgs $H^\pm$ can be written $m^2_{H^\pm} = m_A^2 - \frac{1}{2}(Z_4 - Z_5)v^2$. So we also have

$$m^2_{H^\pm} \simeq m_H^2 - \frac{1}{2}(Z_4 + Z_5)v^2. \tag{5.5}$$

Now, since $|Z_{4,5}| \lesssim \frac{1}{2}$ is required to attain the highest breakdown scales, sufficiently large m_H will lead to mass degenerate BSM Higgs bosons. Indeed, straightforward Taylor expansion in Eqs. (5.4) and (5.5) yields

$$\left|\frac{m_{H^\pm} - m_H}{m_H}\right| \simeq \left|\frac{m_A - m_H}{m_H}\right| \lesssim \left(\frac{v}{2m_H}\right)^2, \tag{5.6}$$

which is valid for $m_H < \frac{v}{2} \approx 120\,\text{GeV}$. Therefore, if we require a high breakdown scale for a 2HDM with a softly broken $\mathbb{Z}_2$ symmetry and $m_H \gtrsim v$ then all the BSM Higgs particles are nearly degenerate in mass.

Finally, let us look at the influence of $\tan\beta$. Comparing Fig. 3, 4 and 5 one can see that the correlations are similar for $\tan\beta = 1.1$, 5 and 25. For $\tan\beta = 1.1$ and $\tan\beta = 5$, the correlations are almost identical. For $\tan\beta = 25$, however, the regions of well-behaved models are much smaller. To evolve up to $10^{16}\,\text{GeV}$, a model must have $|Z_7| \lesssim 0.1$. We conclude that models with large $\tan\beta$ are most constrained by RG evolution.

5.1.2 Exact $\mathbb{Z}_2$ Symmetry

Let us now study the RG evolution of a 2HDM with an exact $\mathbb{Z}_2$ symmetry. When the $\mathbb{Z}_2$ symmetry is exact Z_7 is no longer free and can be expressed in the hybrid basis as [9]

$$Z_7 = \frac{m_h^2 - m_H^2}{v^2} c_{\beta-\alpha} s_{\beta-\alpha} + \frac{2}{v^2} \cot 2\beta \left(m_h^2 c_{\beta-\alpha} + m_H^2 s_{\beta-\alpha}^2 \right). \tag{5.7}$$

Therefore we only need to scan over $\{m_H, \cos(\beta-\alpha), Z_4, Z_5\}$. Having an exact $\mathbb{Z}_2$ symmetry also means that we have no control over the magnitude of Z_7. However, we have seen in Sect. 5.1.1 that a small $|Z_7|$ is critical to achieve a high breakdown scale. Hence an exact $\mathbb{Z}_2$ might severely constrain the parameter space regions of well behaved models. To investigate this possibility we have plotted the Eq. (5.7) for $\tan\beta = 1.1$ and 5 in Fig. 6.

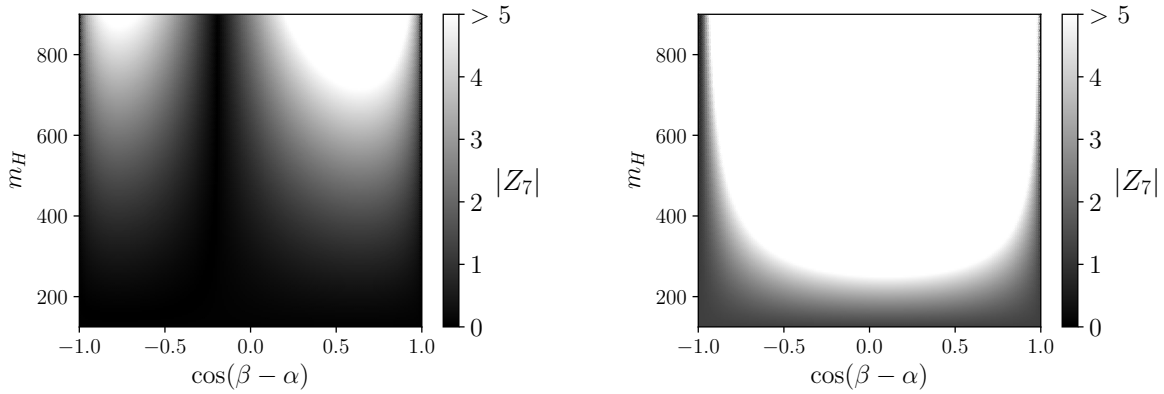

Figure 6: Magnitude of $|Z_7|$ in models with an exact $\mathbb{Z}_2$ symmetry. (left) $\tan\beta = 1.1$ (right) $\tan\beta = 5$.

It is clear that an exact $\mathbb{Z}_2$ symmetry makes it harder to evolve models. This is especially true for large values of $\tan\beta$. When $\tan\beta = 5$, the region of small $|Z_7|$ is extremely limited. In fact, over the range $(m_H, c_{\beta-\alpha}) \in [125, 900] \times [-1, 1]$ we have have $|Z_7| \gtrsim 0.7$. From Fig. 4 we can conclude that models with an exact $\mathbb{Z}_2$ symmetry and $\tan\beta = 5$ can hardly be evolved beyond the top mass. The situation is even worse for $\tan\beta = 25$, in that case we find $|Z_7| \gtrsim 6$. We noted in Fig. 5 that models with $\tan\beta = 25$ require $|Z_7| \lesssim 0.1$ to be

evolved above the top mass scale. Therefore, an exact $\mathbb{Z}_2$ symmetry makes it impossible to evolve such models beyond the top mass scale.

If an exact symmetry is enforced, then $\tan\beta$ must be close to 1. Indeed Fig. 6 shows that for $\tan\beta = 1.1$ one retains significant regions where $|Z_7|$ is small. By virtue of this fact we were only able to perform scans and find models that can be evolved beyond the top mass scale when $\tan\beta = 1.1$.

We display the correlations between parameters in Fig. 7. First we observe that there are no points with a breakdown scale higher than $\sim 10^{13}\,\text{GeV}$. Moreover the correlations between parameters are qualitatively different from the case of softly broken $\mathbb{Z}_2$ symmetry. In this scenario, the masses of the scalars are much more constrained. For example, m_H must be small in order to reach high breakdown scales. We also see that RG evolution seems to favour negative values of $\cos(\beta - \alpha)$.

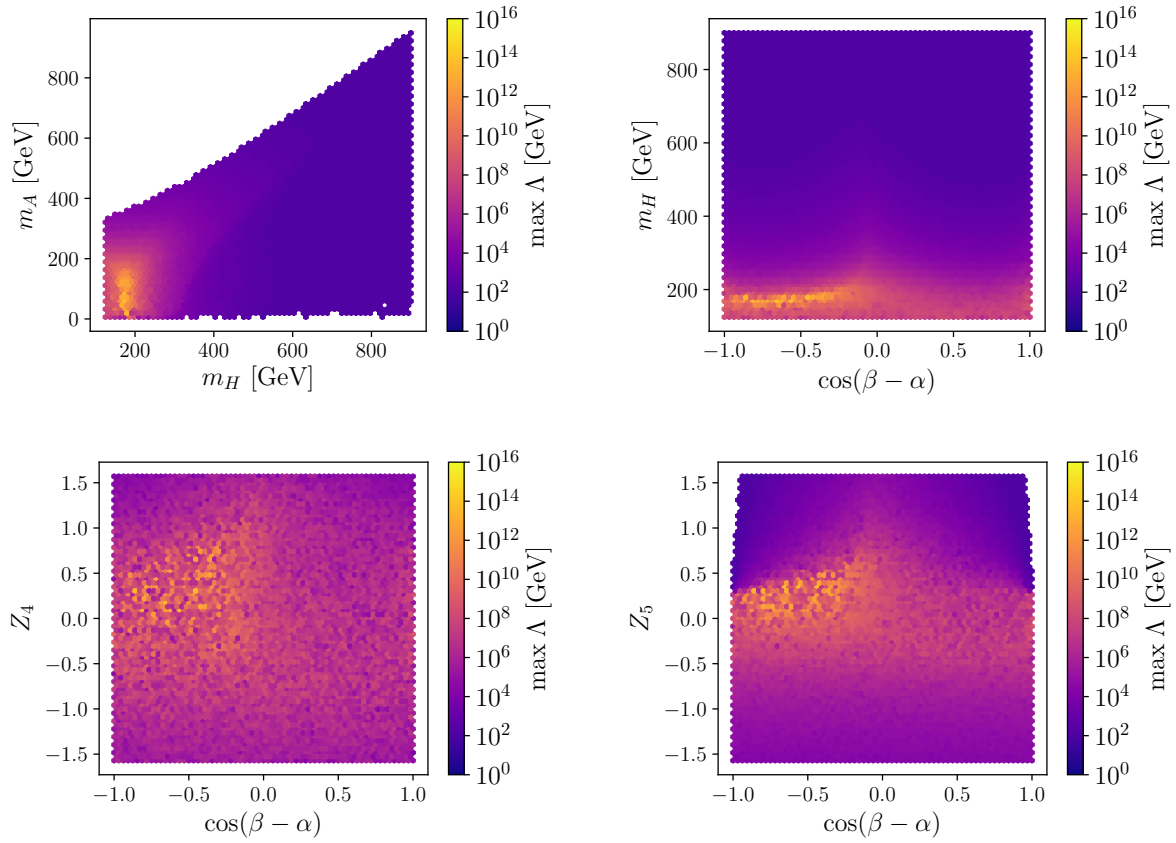

Figure 7: The breakdown scale as a function of 2HDM parameters for the case of an exact $\mathbb{Z}_2$ symmetry and $\tan\beta = 1.1$. We plot the maximum breakdown scale attained in each bin.

5.2 Experimental Constraints

To further constrain the models we apply experimental constraints from Higgs searches at LEP, Tevatron and the LHC using `HiggsBounds`[27] (HB) and `HiggsSignal`[28] (HS). HB subjects the observables predicted by a given model to the experimental limits from searches and determines if the parameter point is excluded with 95% confidence level. HS calculates the goodness of fit of a model, that is how well it reproduces the observed signal. Both programs take as inputs the masses of Higgs bosons, their branching ratios and production cross sections. We use the `C++` program `2HDMC` [29] to generate the input for a 2HDM specified in the hybrid basis and feed it to HB and HS to check experimental constraints.

5.3 Scenario A: $\Lambda_{FN} = 10^5\,\text{GeV}$, Exact $\mathbb{Z}_2$ Symmetry

In this section, we explore the possibility that the FN scale Λ_{FN} is close to 100 TeV. In fact, Λ_{FN} can hardly be lower than 100 TeV since mass scales up to 10 TeV have been explored in experiments and no signs of Froggatt-Nielsen physics have been seen. For example, the constraint from Z' searches is $M_{Z'} \gtrsim 1\,\text{TeV}$ [11]. If the $U(1)'$ coupling is not tiny (say $g' \gtrsim 0.01$), this means that $M_{Z'} \approx \varepsilon g' \Lambda_{FN} \gtrsim 1\,\text{TeV}$ and thus $\Lambda_{FN} \gtrsim 500\,\text{TeV}$. In this scenario one can have an exact $\mathbb{Z}_2$ symmetry while retaining significant portions of parameter space with viable models, however $\tan\beta$ has to be close to 1 as shown in Sect. 5.1.2.

5.3.1 Froggatt-Nielsen Charge Assignment

We now attempt to make charge assignments for these models. To do so we have gathered a sample of $\mathcal{O}(10^5)$ models that breakdown above $10^5\,\text{GeV}$ for each 2HDM type. From Sect. 5.1.2 we know that models with an exact $\mathbb{Z}_2$ symmetry and a breakdown scale above $10^5\,\text{GeV}$ require $\tan\beta \approx 1$. Therefore we only consider the case $\tan\beta = 1.1$ here. We calculate the fermion masses at $\mu = 10^5\,\text{GeV}$ for each point in each sample using `2HDME` and then compute the number of flavon insertions n_i^F needed to account for the value of the masses using Eq. (3.7) and construct the mass constraints. In each sample of points the variation of n_i^F is very small. We can quantify this observation with the maximum relative standard deviation over all samples $\frac{\Delta n_3^U}{\langle n_3^U \rangle} \sim 1\%$. The variations related to the 2HDM type are larger hence we must consider four distinct charge assignments. The numerical values of n_i^F for each 2HDM type are shown in Table 3. We keep three digits to show the small variation due the 2HDM type. The variation is small here since $\tan\beta = \frac{v_2}{v_1} = 1.1$ and thus $v_2 \approx v_1$. The number of flavon insertions must of course be integer so the entries of Table 3 will have to be rounded. Recall that rounding to the closest integer corresponds to choosing the $\mathcal{O}(1)$ coupling g_i^F in Eq. (3.7) in the range $[\varepsilon^{\frac{1}{2}}, \varepsilon^{-\frac{1}{2}}]$.

From Table 3, the mass constraints can be read off by rounding each n_i^F and plugging it in Eq. (3.7). For example, we can write the mass constraints for a type I model with

$\tan\beta = 1.1$ as

$$\begin{aligned}
&Q_1 - u_1 - \chi_1 = n_1^U = 7 \quad Q_2 - u_2 - \chi_1 = n_2^U = 3 \quad Q_3 - u_3 - \chi_1 = n_3^U = 0, \\
&Q_1 - d_1 + \chi_1 = n_1^D = 7 \quad Q_2 - d_2 + \chi_1 = n_2^D = 5 \quad Q_3 - d_3 + \chi_1 = n_3^D = 3, \\
&L_1 - e_1 + \chi_1 = n_1^L = 8 \quad L_2 - e_2 + \chi_1 = n_2^L = 4 \quad L_3 - e_3 + \chi_1 = n_3^L = 3.
\end{aligned} \tag{5.8}$$

For each 2HDM type we look for anomaly free sets of flavon charges satisfying the appropriate mass constraints and the CKM constraints using `Sage`.

The generic system of polynomial equations to be solved is

$$\begin{cases}
\mathcal{A}_{11'1'} \propto \sum_i^3 \left(Q_i^2 - 2u_i^2 + d_i^2 - L_i^2 + e_i^2\right) = 0, \\
\mathcal{A}_{111'} \propto \sum_i^3 \left(Q_i + 8u_i + 2d_i + 3L_i + 6e_i\right) = 0, \\
\mathcal{A}_{331'} \propto \sum_i^3 \left(2Q_i + u_i + d_i\right) = 0, \\
\mathcal{A}_{221'} \propto \sum_i^3 \left(3Q_i + L_i\right) = 0, \\
Q_1 - u_1 - \chi_u = n_1^U, \quad Q_2 - u_2 - \chi_u = n_2^U, \quad Q_3 - u_3 - \chi_u = n_3^U, \\
Q_1 - d_1 + \chi_d = n_1^D, \quad Q_2 - d_2 + \chi_d = n_2^D, \quad Q_3 - d_3 + \chi_d = n_3^D, \\
L_1 - e_1 + \chi_l = n_1^L, \quad L_2 - e_2 + \chi_l = n_2^L, \quad L_3 - e_3 + \chi_l = n_3^L, \\
Q_1 - Q_2 = 1, \\
Q_2 - Q_3 = 2.
\end{cases} \tag{5.9}$$

We will call a set of $U(1)'$ charges satisfying Eqs. 5.9 a valid charge assignment. It was shown in [12] that the anomaly cancellation conditions can be combined to yield the following sum rules for each type of $\mathbb{Z}_2$ symmetry

$$\sum_{i=1}^{3}(n_i^D - n_i^L) = 0 \qquad \text{type II}, \tag{5.10}$$

$$\sum_{i=1}^{3}(n_i^U + n_i^D) = 0 \qquad \text{type X}, \tag{5.11}$$

$$\sum_{i=1}^{3}(n_i^U + n_i^L) = 0 \qquad \text{type Y}. \tag{5.12}$$

Notice that if two fermion species couple to the same Higgs doublet then there is a sum rule relating their flavon insertions. Hence for type I, all three sum rules must be satisfied. These are necessary conditions for a set of charges to be anomaly free.

Type \ $\tan\beta$	1.1		
I	7.33	3.49	-0.06
	6.82	4.99	2.58
	7.69	4.36	2.60
II	7.33	3.49	-0.06
	6.86	5.04	2.55
	7.73	4.41	2.65
X	7.33	3.49	-0.06
	6.82	4.99	2.58
	7.73	4.41	2.65
Y	7.33	3.49	-0.06
	6.86	5.04	2.55
	7.69	4.36	2.60

Table 3: Average ε order of magnitude of the diagonal Yukawa couplings at $\mu = 10^5\,\text{GeV}$ for each 2HDM type and $\tan\beta$ sample. The values are arranged as a matrix $|n_i^F|$ where $F = U, D, L$ is the row index and $i = 1, 2, 3$ is the column index labeling the generations.

It can readily be seen from the sum rules (5.11) and (5.12) that type I, X and Y will require some n_i^F to be negative. Recall that these then correspond to the number of S^* insertions in the FN mechanism. As we will see this usually compromises the ordering in the Yukawa coupling matrices.

Type I models From the above considerations we expect the charge assignment to be most difficult for type I models. Not only are there three sum rules to satisfy but two of them require S^* insertions which could compromise the ordering of the Yukawa coupling matrices and make the FN mechanism inconsistent. In fact, we have not been able to find a set of n_i^F that satisfies the sum rules and produces realistic orders of magnitude for the masses. This means that type I models, and hence the SM, cannot accommodate a FN mechanism. One could of course find a set of flavon insertions satisfying all three sum rules but this would require fine tuning of the couplings g_i^F well outside $\mathcal{O}(1)$.

Type X models For type X models, the sum rule Eq. (5.11) is not satisfied when rounding the entries of Table. 3 to the nearest integer. However if we take $n_3^D = 2$ then the sum rule can be satisfied. This corresponds to choosing $g_3^D = \varepsilon^{0.58} \approx 0.4$ since $Y_3^D = g_3^D \varepsilon^{n_3^D} = \varepsilon^{2.58}$. Although we set out to take the $\mathcal{O}(1)$ couplings $g_i^F \in [\varepsilon^{\frac{1}{2}}, \varepsilon^{-\frac{1}{2}}]$, this small concession preserves $g_3^D \sim \mathcal{O}(1)$ and hence does not introduce inconsistencies in the FN

framework. Thus we find that the flavon insertions

$$\begin{aligned} n_1^U &= 7, \quad & n_2^U &= 3, \quad & n_3^U &= 0, \\ n_1^D &= -7, \quad & n_2^D &= -5, \quad & n_3^D &= 2, \\ n_1^L &= 8, \quad & n_2^L &= 4, \quad & n_3^L &= 3 \end{aligned} \tag{5.13}$$

satisfy the sum rule Eq. (5.11) and produce the correct orders of magnitude for the masses. The Gröbner basis found in `Sage` and the corresponding charges are displayed in Appendix B. These solutions define a hyperplane parametrized by 3 charges, say χ_2, d_3, e_3 and any given choice of these three charges will yield a valid charge assignment. In Table 4 we show the charge assignment obtained for $\chi_2 = d_3 = e_3 = 0$.

χ_2	e_3	d_3	Q_1	Q_2	Q_3	u_1	u_2	u_3	d_1	d_2	L_1	L_2	L_3	e_1	e_2	χ_1
0	0	0	5	4	2	2	-1	-2	-12	-9	$\frac{1}{3}$	-28	$-\frac{16}{3}$	$-\frac{2}{3}$	$\frac{71}{3}$	$-\frac{25}{3}$

Table 4: A valid charge assignment for type X models with $\tan\beta = 1.1$.

We note that, as discussed in [12], when $\chi_2 - \chi_1 \notin \mathbb{Z}$ as is the case for the charge assignment in Table 4, the $\mathbb{Z}_2$ symmetry arises naturally as a remnant of the $U(1)'$ symmetry.

Using these flavon charges and Eq. (3.3) one can calculate the Yukawa couplings generated by the FN mechanism

$$Y^U \sim \begin{pmatrix} \varepsilon^7 & \varepsilon^4 & \varepsilon^3 \\ \varepsilon^6 & \varepsilon^3 & \varepsilon^2 \\ \varepsilon^4 & \varepsilon^3 & \varepsilon^0 \end{pmatrix}, \quad Y^D \sim \begin{pmatrix} \varepsilon^7 & \varepsilon^4 & \varepsilon^5 \\ \varepsilon^8 & \varepsilon^5 & \varepsilon^3 \\ \varepsilon^{10} & \varepsilon^7 & \varepsilon^2 \end{pmatrix}, \qquad Y^L \sim \begin{pmatrix} \varepsilon^8 & 0 & 0 \\ 0 & \varepsilon^4 & 0 \\ 0 & 0 & \varepsilon^3 \end{pmatrix}. \tag{5.14}$$

We use $\sim$ as a reminder that we do not write the $\mathcal{O}(1)$ coefficients g_{ij}^F but only the orders of magnitude.

Looking at Eq. (5.14) it is clear that the ordering $n_{i+1,j}^F \leq n_{i,j}^F$ and $n_{i,j+1}^F \leq n_{i,j}^F$ has been compromised in Y^D. The ordering assumption is critical in the FN framework and it would be inconsistent to dismiss it now. The reason is that we have assumed that the masses are given by the diagonal Yukawa couplings (Eq. 3.6) which only follows from the ordering assumption. One might think that the ordering can be fixed by a clever choice of parametrization i.e. a different choice of χ_2, e_3 and d_3, but this is not the case since Y^U and Y^D are completely determined by the mass constraints and the CKM constraints. This can be seen by considering $n_{i\pm1,j}^{U/D} - n_{i,j}^{U/D}$. For instance

$$n_{2,1}^{U/D} - n_{1,1}^{U/D} = Q_2 - Q_1 = -1 \iff |n_{2,1}^{U/D}| = |n_{1,1}^{U/D} - 1|, \tag{5.15}$$

where we have used the formula for n_{ij}^F in Eq. (3.3) and the CKM constraint in Eq. (3.10). Proceeding in a similar manner for all off-diagonal elements, one finds that

$$Y^{U/D} \sim \begin{pmatrix} \varepsilon^{|n_1^{U/D}|} & \varepsilon^{|n_2^{U/D}+1|} & \varepsilon^{|n_3^{U/D}+3|} \\ \varepsilon^{|n_1^{U/D}-1|} & \varepsilon^{|n_2^{U/D}|} & \varepsilon^{|n_3^{U/D}+2|} \\ \varepsilon^{|n_1^{U/D}-3|} & \varepsilon^{|n_2^{U/D}-2|} & \varepsilon^{|n_3^{U/D}|} \end{pmatrix}. \tag{5.16}$$

Therefore type X models are incompatible with the FN mechanism. They cannot both reproduce the fermion masses and mixings and be anomaly free.

Type Y models For type Y models the situation is similar to type X. The sum rule Eq. (5.12) cannot be satisfied unless one allows some small deviations from $g_i^F \in [\varepsilon^{\frac{1}{2}}, \varepsilon^{-\frac{1}{2}}]$. Proceeding analogously as for type X we find that the following flavon insertions

$$\begin{aligned} n_1^U &= 7, \quad n_2^U = 3, \quad n_3^U = 0, \\ n_1^D &= 7, \quad n_2^D = 5, \quad n_3^D = 3, \\ n_1^L &= -8, \quad n_2^L = -4, \quad n_3^L = 2 \end{aligned} \tag{5.17}$$

satisfy the sum rule Eq. (5.12) and produce the correct orders of magnitude for the masses. Again the Gröbner basis and the parametrization of the solutions in terms of the charges χ_2, d_3 and e_3 are displayed in Appendix B. We show one valid charge assignment for this model in Table 5

χ_2	e_3	d_3	Q_1	Q_2	Q_3	u_1	u_2	u_3	d_1	d_2	L_1	L_2	L_3	e_1	e_2	χ_1
0	0	0	$-\frac{7}{3}$	$-\frac{10}{3}$	$-\frac{16}{3}$	$\frac{28}{3}$	$\frac{19}{3}$	$\frac{16}{3}$	1	0	$-\frac{22}{3}$	$\frac{115}{3}$	2	$-\frac{2}{3}$	$-\frac{127}{3}$	$-\frac{25}{3}$

Table 5: A valid charge assignment for type Y models with $\tan\beta = 1.1$.

With these flavon charges, the FN mechanism generates the Yukawa couplings

$$Y^U \sim \begin{pmatrix} \varepsilon^7 & \varepsilon^4 & \varepsilon^3 \\ \varepsilon^6 & \varepsilon^3 & \varepsilon^2 \\ \varepsilon^4 & \varepsilon^3 & \varepsilon^0 \end{pmatrix}, \quad Y^D \sim \begin{pmatrix} \varepsilon^7 & \varepsilon^6 & \varepsilon^6 \\ \varepsilon^6 & \varepsilon^5 & \varepsilon^4 \\ \varepsilon^4 & \varepsilon^3 & \varepsilon^3 \end{pmatrix}, \qquad Y^L \sim \begin{pmatrix} \varepsilon^8 & 0 & 0 \\ 0 & \varepsilon^4 & 0 \\ 0 & 0 & \varepsilon^2 \end{pmatrix}. \tag{5.18}$$

As opposed to type X models the ordering is preserved in the quark Yukawa couplings. This happens because we are able to have all the S^* insertions in the lepton sector where we haven't imposed any mixing constraint.

Type II models For type II models it is remarkable that the sum rule (5.10) is satisfied by rounding the entries of Table 3 to the nearest integer. Moreover because we can take all positive n_i^F the ordering of the Yukawa coupling matrices will be preserved. We find the Gröbner basis in `Sage`. It can be found along with the solutions parametrized by χ_2, d_3 and e_3 in Appendix B. A valid charge assignment is shown in Table 6

χ_2	e_3	d_3	Q_1	Q_2	Q_3	u_1	u_2	u_3	d_1	d_2	L_1	L_2	L_3	e_1	e_2	χ_1
0	0	0	$-\frac{7}{3}$	$-\frac{10}{3}$	$-\frac{16}{3}$	$\frac{28}{3}$	$\frac{19}{3}$	$\frac{16}{3}$	1	0	$\frac{43}{6}$	$\frac{187}{6}$	$-\frac{16}{3}$	$-\frac{15}{2}$	$-\frac{71}{2}$	$-\frac{25}{3}$

Table 6: A valid charge assignment for type II models with $\tan\beta = 1.1$.

With these charges the FN mechanism generates the Yukawa couplings

$$Y^U \sim \begin{pmatrix} \varepsilon^7 & \varepsilon^4 & \varepsilon^3 \\ \varepsilon^6 & \varepsilon^3 & \varepsilon^2 \\ \varepsilon^4 & \varepsilon^3 & \varepsilon^0 \end{pmatrix}, \quad Y^D \sim \begin{pmatrix} \varepsilon^7 & \varepsilon^6 & \varepsilon^6 \\ \varepsilon^6 & \varepsilon^5 & \varepsilon^4 \\ \varepsilon^4 & \varepsilon^3 & \varepsilon^3 \end{pmatrix}, \qquad Y^L \sim \begin{pmatrix} \varepsilon^8 & 0 & 0 \\ 0 & \varepsilon^4 & 0 \\ 0 & 0 & \varepsilon^3 \end{pmatrix}. \tag{5.19}$$

These Yukawa coupling matrices are ordered and therefore the FN framework is consistent in type II models.

To summarize, valid charge assignment leading to ordered Yukawa couplings can be made for both type II and type Y. However it seems that type II is preferred as it doesn't require S^* insertions and one can have $g_i^F \in [\varepsilon^{\frac{1}{2}}, \varepsilon^{-\frac{1}{2}}]$.

5.3.2 Renormalization Group Flow

In this section we study possible physics at the FN scale given that models are well behaved under RG evolution up to $\Lambda_{FN} = 10^5\,\text{GeV}$ and consistent with experimental constraints at the electroweak scale. To do so we consider the flow of these viable models under RG evolution. Specifically, given a viable model at the top mass scale, we are interested in the value of the parameters of the potential at the FN scale $\Lambda_{FN} = 10^5\,\text{GeV}$.

In Sect. 5.1.2 we have found that models with an exact $\mathbb{Z}_2$ symmetry require $\tan\beta \approx 1$ to be well behaved under RG evolution. Moreover in Sect. 5.3.1, we have seen that type II models are best suited to accommodate the FN mechanism. Hence we will focus our analysis on type II models with $\tan\beta = 1.1$. We have gathered a sample of such models of size $\mathcal{O}(10^3)$ by performing scans with `2HDME`. Each parameter space point was subjected to experimental constraints using `HiggsBounds` and `HiggsSignal`. In this section we only consider models consistent with experiments.

In Fig. 8 we have plotted the masses of the BSM Higgs bosons in viable models. Comparing Fig. 7 and Fig. 8 one can see that the experimental constraints further restrict the possible BSM Higgs masses at the top mass scale. Indeed the requirement of good behaviour under RG evolution and the experimental bounds constrain the models to three approximately disjoint regions in the $m_H - m_A - m_{H^\pm}$ hyperplane. Hence we identify three different types of BSM scalar spectrum at the electroweak scale.

We also note that there are no models with $m_H, m_A \gtrsim 300\,\text{GeV}$ at the electroweak scale. This a consequence of the exact $\mathbb{Z}_2$ symmetry since the mass of the pseudoscalar can be written [6]

$$m_A^2 = \frac{m_{12}^2 v^2}{v_1 v_2} - \lambda_5 v^2. \tag{5.20}$$

Hence when the $\mathbb{Z}_2$ symmetry is exact $m_{12}^2 = 0$ and $m_A^2 = -\lambda_5 v^2$. Now, since λ_5 cannot be too large to reach breakdown scales above $10^5\,\text{GeV}$, m_A cannot be too large either. Moreover, since m_A^2 is the main contribution to m_H^2 (see Eq. (2.10)), the exact $\mathbb{Z}_2$ symmetry also restricts how heavy H can be.

At 10^5 GeV, the masses have increased due to the growth of the quartic couplings. The shape of the $m_H - m_A - m_{H^\pm}$ regions of viable models changes and some correlations arise. For example, at 10^5 GeV many models lie in the region $m_H \approx 2m_A \approx m_{H^\pm}$.

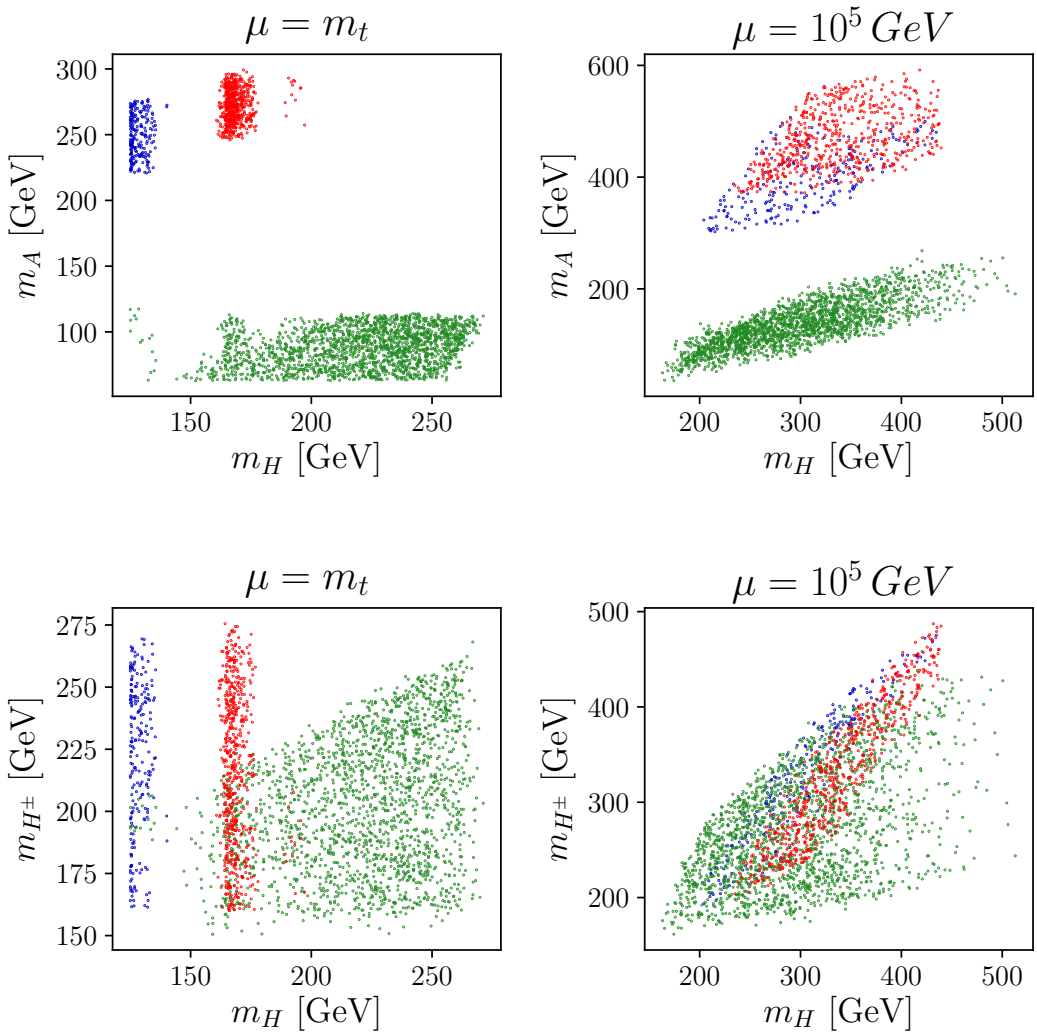

Figure 8: Top-left: $m_H - m_A$ plane of the region of well behaved models consistent with experiments at the top mass scale m_t. Top-right: same region evolved to $\mu = 10^5$ GeV. Bottom-left: $m_H - m_{H^\pm}$ plane of the region of well behaved models consistent with experiments at the top mass scale m_t. Bottom-right: same region evolved to $\mu = 10^5$ GeV. Color scheme: red: $m_A(m_t) < 200$ GeV and $m_H(m_t) < 150$ GeV; blue: $m_A(m_t) < 200$ GeV and $m_H(m_t) \geq 150$ GeV; green: $m_A(m_t) \leq 200$ GeV

Fig. 9 shows the region of viable models in the $c_{\beta-\alpha} - m_H$ plane at the top mass scale and at the FN scale. Since the coupling of h (H) to the $W^\pm$ and Z^0 is proportional to $s^2_{\beta-\alpha}$ ($c^2_{\beta-\alpha}$) [26], the central region with $-0.25 < c_{\beta-\alpha} < 0.25$ correspond to models

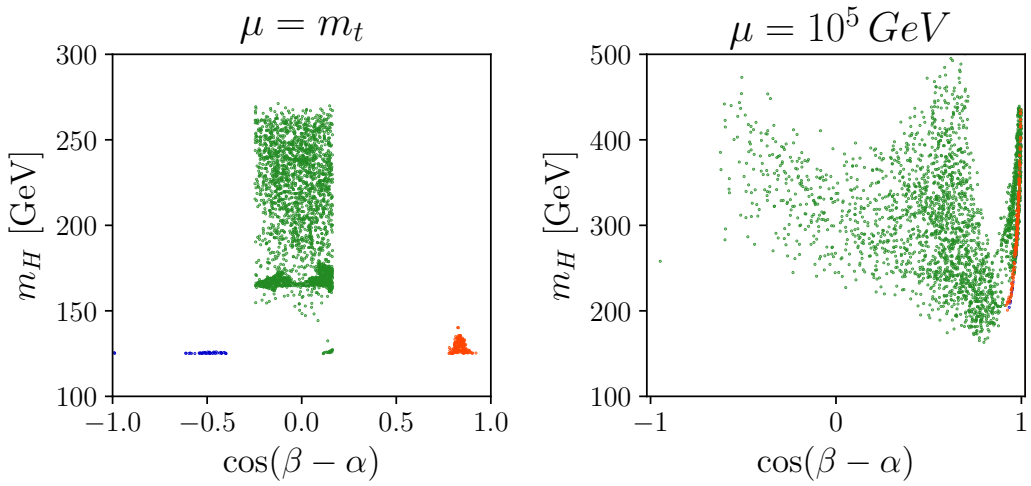

Figure 9: Left: $c_{\beta-\alpha} - m_H$ plane of the region of well behaved models consistent with experiments at the top mass scale m_t. Right: same region evolved to $\mu = 10^5$ GeV. Color scheme: blue: $c_{\beta-\alpha}(m_t) < -0.3$; green: $-0.3 \geq c_{\beta-\alpha}(m_t) \leq 0.3$; red: $c_{\beta-\alpha}(m_t) > 0.3$

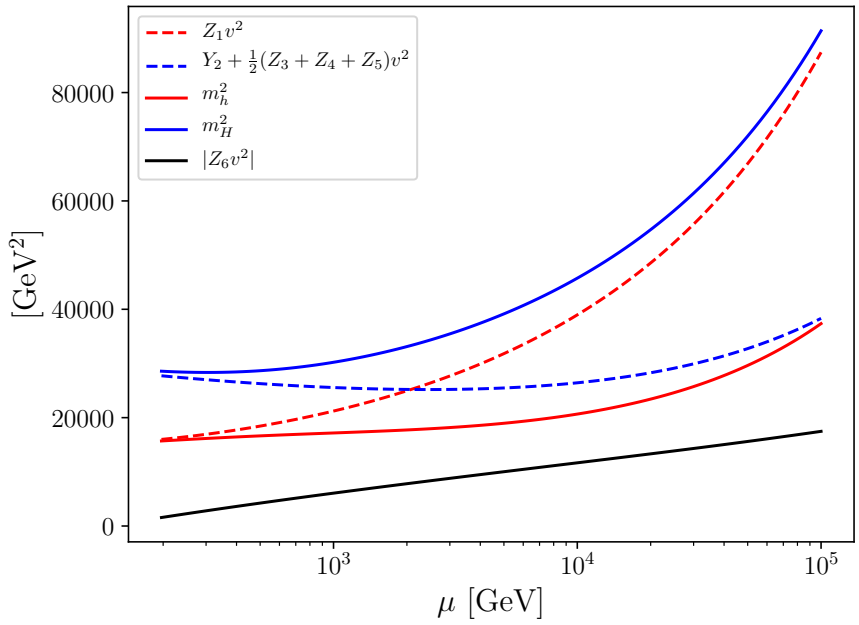

Figure 10: RG evolution of a point with $c_{\beta-\alpha}(\mu = m_t) = 0.09$ and $c_{\beta-\alpha}(\mu = 10^5\,\text{GeV}) = 0.94$. At the top mass scale m_t, $m_h^2 = Z_1 v^2$ and $m_H^2 = Y_2 + \frac{1}{2}(Z_3 + Z_4 + Z_5)v^2$. At 10^5 GeV these relations have swapped due to the growth of $Z_1 v^2$ and the definition $m_H \geq m_h$.

where the observed Higgs is h. The other allowed regions have larger values of $c_{\beta-\alpha}$ and $m_H \approx m_h \approx 125\,\text{GeV}$ and thus correspond to models where H is the main contribution to the observed Higgs.

It is interesting to consider how these regions flow under RG evolution. First it can be seen that generally $c_{\beta-\alpha}$, and hence the coupling of H with vector bosons, increases with the energy scale. That means it is possible to have models where at the top mass scale the vector bosons mostly couple with the light Higgs h but at $10^5\,\text{GeV}$ the vector bosons mostly couple to the heavier Higgs H.

We can trace the origin of the growth of $c_{\beta-\alpha}$ by considering the mass matrix in Eq. (2.8). Since $\beta-\alpha$ is the rotation angle that diagonalizes this mass matrix, $c_{\beta-\alpha}=0$ means that the Higgs basis and the mass basis coincide, i.e. the mass matrix is diagonal in the Higgs basis. In that case $m_h^2 = Z_1 v^2$ and $m_H^2 = Y_2 + \frac{1}{2}(Z_3+Z_4+Z_5)v^2$. However during RG evolution it can happen that $Z_1 v^2$ becomes larger than $Y_2 + \frac{1}{2}(Z_3+Z_4+Z_5)v^2$. Then, since by definition $m_H \geq m_h$, one has $m_H^2 = Z_1 v^2$. This corresponds to swapping the mass eigenstates and hence to $c_{\beta-\alpha}=1$. This is illustrated in Fig. 10.

We have made the assumptions that the electroweak scale physics is described by a 2HDM with an exact $\mathbb{Z}_2$ symmetry which is the low energy limit of a theory defined at $\Lambda_{FN} = 10^5\,\text{GeV}$. This allowed us to constrain the models at Λ_{FN}. We found that the exact $\mathbb{Z}_2$ constrains the BSM Higgs masses to be less than $\sim 500\,\text{GeV}$. We also found that for many models the weak bosons couple to the light Higgs scalar at the electroweak scale but they couple to the heavy Higgs scalar at the FN scale.

5.4 Scenario B: $\Lambda_{FN} = 10^{16}\,\text{GeV}$, Softly Broken $\mathbb{Z}_2$ Symmetry

In this section we explore models with a FN scale close to the GUT scale. This is about as high as the FN scale can be. Indeed higher scales approach the Planck scale $\Lambda_\text{P} \sim 10^{19}\,\text{GeV}$ where quantum gravity is expected to become relevant so it might not make sense to look for a quantum field theory there.

It was shown in [19] that while an exact $\mathbb{Z}_2$ symmetry severely constrains the regions of parameter space that can be evolved up to $10^{16}\,\text{GeV}$, a softly broken $\mathbb{Z}_2$ symmetry allows larger regions of viable models. Therefore we use a softly broken $\mathbb{Z}_2$ symmetry for the models with $\Lambda_{FN} = 10^{16}\,\text{GeV}$.

5.4.1 Froggatt-Nielsen Charge Assignment

We now search for Froggatt-Nielsen charge assignments for the models at hand. The number of flavon insertions needed to account for the masses at $\Lambda_{FN} = 10^{16}\,\text{GeV}$ can be computed as in Eq. (3.7). From the scans with `2HDME`, we have gathered samples of points that can evolve up to $10^{16}\,\text{GeV}$ for types I, II, X and Y and $\tan\beta = 1.1, 5, 25$. While for $\tan\beta = 5$ and 25 the size of the samples are $\mathcal{O}(10^4)$, we only find a handful of points with $\tan\beta = 1.1$. We suppose that models with $\tan\beta = 1.1$ require a larger degree of fine tuning between their parameters to reach a breakdown scale of $10^{16}\,\text{GeV}$. Nevertheless, we compute the average number of flavon insertions for each point in each

(type, $\tan\beta$) sample. The results are shown in Table 7. We again observe that the variation of the number of flavon insertions over a given sample of points is very small. Over the 12 samples, the maximum relative standard deviation $\frac{\Delta n}{\langle n\rangle}$ occurs for the top quark and is of order $\frac{\Delta n_3^U}{\langle n_3^U\rangle} \sim 1\%$. This very small influence of the scalar sector on the running of the fermion masses is expected since the scalar parameters enter the Yukawa RG equations at 2-loop. Therefore there are only 12 distinct flavon charge assignments to consider.

In this scenario we actually have to consider different values of $\tan\beta$. Let us therefore make explicit the baseline dependence of the mass constraints on 2HDM type and $\tan\beta$. We rewrite the number of flavon insertions as

$$n_i^F = \begin{cases} \log_\varepsilon\left(Y^F_{1,ii}\right) = \log_\varepsilon\left(\frac{\sqrt{2}m_i^F}{v\cos\beta}\right), & F \text{ couples to } \Phi_1 \\ \log_\varepsilon\left(Y^F_{2,ii}\right) = \log_\varepsilon\left(\frac{\sqrt{2}m_i^F}{v\sin\beta}\right), & F \text{ couples to } \Phi_2 \end{cases}. \tag{5.21}$$

Note that the appearance of $v_1 = v\cos\beta$ and $v_2 = v\sin\beta$ in these expressions implies that the mass constraints are different for each 2HDM type and $\tan\beta$. It also introduces an additional scale dependence through the running of v_1 and v_2 (or equivalently through the running of $\tan\beta$ and v). The values 5 and 25 where chosen because they can be expressed as ε^{-k} with $k = 1$ and $k = 2$ respectively. For these large values of $\tan\beta$ we have $\tan\beta \approx \frac{1}{\cos\beta} = \varepsilon^{-k}$ and $\sin\beta \approx 1$. Therefore Eq. (5.21) simplifies to

$$n_i^F = \begin{cases} \log_\varepsilon\left(\frac{\sqrt{2}m_i^F}{v}\right) - k, & F \text{ couples to } \Phi_1 \\ \log_\varepsilon\left(\frac{\sqrt{2}m_i^F}{v}\right), & F \text{ couples to } \Phi_2 \end{cases}. \tag{5.22}$$

That explains the variation $|n_i^F| \to |n_i^F| - 1$ in Table 7 for fermions coupling to Φ_1 when going from $\tan\beta = 5$ to $\tan\beta = 25$. Physically, when $\tan\beta = \frac{v_2}{v_1}$ grows this means that v_1 decreases and hence the Yukawa couplings of fermions coupling to Φ_1 must increase to keep the mass constant.

Once Table 7 has been stripped from the preceding baseline dependence on $\tan\beta$ and the 2HDM type it can be seen that the residual effect on the running of the masses due $\tan\beta$ and the 2HDM type first affects n_i^F in the second and third digit, respectively. That is, $\tan\beta$ and the 2HDM type have little influence on the running of the masses.

We proceed to investigate whether valid charge assignments can be made for each of the 12 distinct models considered.

Type I models In fact if the n_i^F in Table 7 are rounded to the nearest integer, there is no way to satisfy the sum rules for type I, even when allowing S^* insertions. For this type, a valid FN charge assignment would require the g_{ij}^F to be taken well outside the range $[\varepsilon^{\frac{1}{2}}, \varepsilon^{-\frac{1}{2}}]$. Again, this introduces inconsistencies with the original assumptions of the FN mechanism i.e. all the g_{ij}^F are assumed to be of the same order of magnitude $\mathcal{O}(1)$. Therefore if a type I 2HDM is to be equipped with a gauged FN mechanism then the original assumption of Froggatt and Nielsen must be relaxed. This makes such models less attractive.

Type \ $\tan\beta$	1.1			5			25		
I	7.44	3.60	-0.11	7.92	4.08	0.52	7.94	4.10	0.54
	6.91	5.09	2.85	7.39	5.57	3.18	7.41	5.59	3.19
	7.48	4.15	2.39	7.96	4.63	2.87	7.98	4.65	2.89
II	7.44	3.60	-0.11	7.92	4.08	0.51	7.94	4.10	0.53
	7.31	5.48	2.94	6.48	4.66	2.17	5.53	3.70	1.20
	7.87	4.55	2.78	7.05	3.72	1.96	6.09	2.76	0.99
X	7.44	3.60	-0.11	7.92	4.08	0.52	7.94	4.10	0.54
	6.91	5.09	2.85	7.39	5.57	3.18	7.41	5.59	3.19
	7.87	4.54	2.78	7.10	3.78	2.02	6.11	2.78	1.01
Y	7.44	3.60	-0.11	7.92	4.08	0.52	7.94	4.10	0.53
	7.31	5.48	2.95	6.54	4.72	2.23	5.53	3.71	1.21
	7.48	4.15	2.39	7.96	4.63	2.87	7.97	4.65	2.89

Table 7: Average ε order of magnitude of the diagonal Yukawa couplings at $\mu = 10^{16}$ GeV for each 2HDM type and $\tan\beta$ sample. The values are arranged as a matrix $|n_i^F|$ where $F = U, D, L$ is the row index and $i = 1, 2, 3$ is the column index labeling the generations.

Type X models Let us now consider type X. For $\tan\beta = 5$ and $\tan\beta = 25$ we can choose the n_i^F so as to satisfy the sum rule in Eq. (5.11). For $\tan\beta = 5$, one possibility is to have

$$\begin{aligned} n_1^U &= -8, \quad n_2^U = 4, \quad n_3^U = 0, \\ n_1^D &= 7, \quad n_2^D = -6, \quad n_3^D = 3, \\ n_1^L &= 7, \quad n_2^L = 4, \quad n_3^L = 2. \end{aligned} \tag{5.23}$$

Therefore there is a chance to make a valid charge assignment with the corresponding mass constraints. Indeed, for this particular choice we find the Gröbner basis using `Sage`. It is given, along with the parametrization of the solutions in terms of χ_2, e_3 and d_3 in Appendix C. For definiteness, we show one set of solutions in Table 8.

χ_2	e_3	d_3	Q_1	Q_2	Q_3	u_1	u_2	u_3	d_1	d_2	L_1	L_2	L_3	e_1	e_2	χ_1
0	0	0	6	5	3	-14	-1	-3	1	11	$-\frac{61}{3}$	$-\frac{62}{3}$	-1	$\frac{73}{3}$	$\frac{65}{3}$	-3

Table 8: A valid charge assignment for type X with $\tan\beta = 5$.

The charge assignment for models with $\tan\beta = 25$ is completely analogous so we do not present it here (the Gröbner basis and parametrized solutions can be found in Appendix C).

The charge assignment in Table 8 has the interesting feature that $\chi_2 - \chi_1 = 3$ is an integer. As a consequence the $\mathbb{Z}_2$-breaking term

$$S^3 \Phi_2^\dagger \Phi_1 \tag{5.24}$$

is gauge invariant. Therefore, in this model, the $\mathbb{Z}_2$ symmetry cannot be regarded as a remnant of the $U(1)'$ symmetry as before. In that case, one has to impose the $\mathbb{Z}_2$ symmetry by hand which makes such models less attractive.

The FN mechanism with the above charges generates the following Yukawa couplings.

$$Y^U \sim \begin{pmatrix} \varepsilon^8 & \varepsilon^5 & \varepsilon^3 \\ \varepsilon^9 & \varepsilon^4 & \varepsilon^2 \\ \varepsilon^{11} & \varepsilon^2 & \varepsilon^0 \end{pmatrix}, \quad Y^D \sim \begin{pmatrix} \varepsilon^7 & \varepsilon^5 & \varepsilon^6 \\ \varepsilon^6 & \varepsilon^6 & \varepsilon^5 \\ \varepsilon^4 & \varepsilon^8 & \varepsilon^3 \end{pmatrix}, \qquad Y^L \sim \begin{pmatrix} \varepsilon^8 & 0 & 0 \\ 0 & \varepsilon^5 & 0 \\ 0 & 0 & \varepsilon^3 \end{pmatrix}. \tag{5.25}$$

These Yukawa coupling matrices are not ordered. Therefore the Froggatt-Nielsen mechanism is inconsistent in type X models.

Type Y models One can arrange similarly a valid charge assignment in type Y models. In models with $\tan\beta = 1.1$, the following flavon insertions satisfy the sum rule in Eq. (5.12)

$$\begin{aligned} n_1^U &= -8, \quad n_2^U = 3, \quad n_3^U = 0, \\ n_1^D &= 7, \quad n_2^D = 5, \quad n_3^D = 3, \\ n_1^L &= 7, \quad n_2^L = -4, \quad n_3^L = 2. \end{aligned} \tag{5.26}$$

This requires relaxing our assumption that $g_i^F \in [\varepsilon^{\frac{1}{2}}, \varepsilon^{-\frac{1}{2}}]$. In this model one would have $g_1^U = \varepsilon^{-0.56} \approx 2.5$ and $g_2^U = \varepsilon^{0.60} \approx 0.4$ as can be verified in Table 7. Again, these are small concessions and it is not unreasonable to claim that these numbers are still $\mathcal{O}(1)$. Hence we proceed and find the Gröbner basis for the corresponding system of equations. It is given in Appendix C with the parametrization of the solutions. We show one valid charge assignment in Table 9.

χ_2	e_3	d_3	Q_1	Q_2	Q_3	u_1	u_2	u_3	d_1	d_2	L_1	L_2	L_3	e_1	e_2	χ_1
0	0	0	$\frac{20}{3}$	$\frac{17}{3}$	$\frac{11}{3}$	$\frac{44}{3}$	$-\frac{8}{3}$	$-\frac{11}{3}$	1	1	$-\frac{989}{33}$	$\frac{667}{33}$	2	$\frac{1214}{33}$	$\frac{535}{33}$	$\frac{20}{3}$

Table 9: A valid charge assignment for type Y with $\tan\beta = 1.1$.

With these charges, the Yukawa couplings are

$$Y^U \sim \begin{pmatrix} \varepsilon^8 & \varepsilon^4 & \varepsilon^3 \\ \varepsilon^9 & \varepsilon^3 & \varepsilon^2 \\ \varepsilon^{11} & \varepsilon^1 & \varepsilon^0 \end{pmatrix}, \quad Y^D \sim \begin{pmatrix} \varepsilon^7 & \varepsilon^6 & \varepsilon^6 \\ \varepsilon^6 & \varepsilon^5 & \varepsilon^5 \\ \varepsilon^4 & \varepsilon^3 & \varepsilon^3 \end{pmatrix}, \qquad Y^L \sim \begin{pmatrix} \varepsilon^7 & 0 & 0 \\ 0 & \varepsilon^4 & 0 \\ 0 & 0 & \varepsilon^2 \end{pmatrix}. \tag{5.27}$$

Notice that the ordering of the Y^U has been compromised. However the terms that break the ordering are very small, hence they are negligible in diagonalization procedure. Note also that due to n_2^L being negative, if one were to include any lepton mixing then the ordering of Y^L would likely be lost. Hence these models are viable in this limited framework but would not work in a more realistic setting with neutrino masses and lepton mixing.

Type II models The sum rule for type II in Eq. (5.10) can be satisfied with positive n_i^F. We note in passing that this sum rule is the form of the Georgi-Jarlskog mass relations [30] in this model i.e.

$$n_1^D - n_1^L + n_2^D - n_2^L + n_3^D - n_3^L = 0 \iff 1 = \frac{\varepsilon^{n_1^D}\varepsilon^{n_2^D}\varepsilon^{n_3^D}}{\varepsilon^{n_1^L}\varepsilon^{n_2^L}\varepsilon^{n_3^L}} \approx \frac{m_d m_s m_b}{m_e m_\mu m_\tau}. \tag{5.28}$$

For $\tan\beta = 5$ the sum rule is satisfied when the n_i^F in Table 7 are rounded to the nearest integer. For $\tan\beta = 1.1$ and $\tan\beta = 25$ one again has to make small concessions and choose the g_i^F outside $[\varepsilon^{\frac{1}{2}}, \varepsilon^{-\frac{1}{2}}]$. For these three cases we find Gröbner bases in `Sage`. They can be found in Appendix C. For $\tan\beta = 5$ and $\tan\beta = 25$, the Gröbner bases are the same except for the equations relating χ_1 and χ_2. The reason for this is that $\tan\beta$ only modifies the mass constraints of the fermion species that couple to H_1. The change in the number of flavon insertions due to a change in the value of $\tan\beta$ can therefore be absorbed in a redefinition of χ_1. This relates the Gröbner bases for the different values of $\tan\beta$. The solutions are given in Appendix C. Here we simply show one solution for $\tan\beta = 5$ in Table 10.

χ_2	e_3	d_3	Q_1	Q_2	Q_3	u_1	u_2	u_3	d_1	d_2	L_1	L_2	L_3	e_1	e_2	χ_1
0	0	0	$-\frac{11}{3}$	$-\frac{14}{3}$	$-\frac{20}{3}$	$\frac{35}{3}$	$\frac{26}{3}$	$\frac{23}{3}$	1	1	$\frac{2}{3}$	51	$-\frac{20}{3}$	$-\frac{7}{3}$	$-\frac{167}{3}$	$-\frac{26}{3}$

Table 10: A valid charge assignment for type II with $\tan\beta = 5$. For $\tan\beta = 25$ the same charge assignment is valid with $\chi_1 = -\frac{23}{3}$ instead.

In type II models with $\tan\beta = 5$, the FN mechanism generates the following Yukawa couplings

$$Y^U \sim \begin{pmatrix} \varepsilon^8 & \varepsilon^5 & \varepsilon^4 \\ \varepsilon^7 & \varepsilon^4 & \varepsilon^3 \\ \varepsilon^5 & \varepsilon^2 & \varepsilon^1 \end{pmatrix}, \quad Y^D \sim \begin{pmatrix} \varepsilon^6 & \varepsilon^6 & \varepsilon^5 \\ \varepsilon^5 & \varepsilon^5 & \varepsilon^4 \\ \varepsilon^3 & \varepsilon^3 & \varepsilon^2 \end{pmatrix}, \qquad Y^L \sim \begin{pmatrix} \varepsilon^7 & 0 & 0 \\ 0 & \varepsilon^4 & 0 \\ 0 & 0 & \varepsilon^2 \end{pmatrix}. \tag{5.29}$$

Because it was possible to have all positive n_i^F for these models, the Yukawa coupling matrices are ordered.

In summary, Type II 2HDMs seem to be most compatible with the FN mechanism and anomaly cancellations. In type I, X and Y either the Yukawa matrices cannot be ordered or some large deviations from $g_{ij}^F \in [\varepsilon^{\frac{1}{2}}, \varepsilon^{-\frac{1}{2}}]$ are required.

5.4.2 Renormalization Group Flow

In Sect. 5.1.1 we found regions of models with a softly broken $\mathbb{Z}_2$ that can be evolved up to $\Lambda_{FN} = 10^{16}\,\text{GeV}$. In this section we also require that all the models pass experimental constraints enforced by `HiggsBounds` and `HiggsSignal`. These regions correspond to realistic models at the top mass scale. We now investigate how these models flow under RG

evolution. For this purpose we gathered samples of size $\mathcal{O}(10^3)$ of such models and evolved their parameters up to 10^{16} GeV.

Models with very high breakdown scales require some degree of fine tuning between their parameters. Therefore looking for such models with uniform scans is quite inefficient. To improve the search we take advantage of the correlations found in Sect. 5.1.1 and scan the region

$$\begin{aligned} Z_4 &\in \Big[-0.5, +0.5\Big] & Z_5 &\in \Big[-0.5, +0.5\Big] & Z_7 &\in \Big[-0.5, +0.5\Big] \\ \cos(\beta-\alpha) &\in \Big[-0.25, +0.25\Big] & m_H &\in \Big[125, 1200\Big]\,\text{GeV} \end{aligned}$$

where most of the models with high breakdown scales are. Note that we allow the mass of H to be as high as 1200 GeV. This is motivated by Fig. 4 and 5 where there are well behaved models up to 900 GeV and the observation that experimental constraints favour large masses for the second Higgs scalar.

As mentioned in Sect. 5.4.1, it appears that models with $\tan\beta = 1.1$ require a high degree of fine tuning between their parameters to be evolved up to 10^{16} GeV. Even when taking advantage of the correlations between breakdown scale and the 2HDM parameters, we were not able to find enough points with $\tan\beta = 1.1$ to study the RG flow. For these models a more refined scanning of the parameter space might be necessary. In this section we will therefore only discuss models with $\tan\beta = 5$ and 25.

Investigating the allowed parameter space regions at Λ_{FN} will allow us to probe some of the physics at that scale and connect it to physics at the electroweak scale.

As discussed in Sect. 5.4.1, type II models are best suited to accommodate an anomaly free, realistic FN mechanism. Hence in this section we will restrict our attention to these more promising models.

Fig. 11 shows that the relation $m_A \approx m_H$ found in Sect. 5.1.1 for well behaved models still holds at 10^{16} GeV. The similar relation $m_{H^\pm} \approx m_H$ also holds at that scale but we do not plot it here. These relations are consequences of the requirement of RG evolution up to 10^{16} GeV which is quite strong and constrains the quartic couplings to be small throughout the evolution. As a result Eq. (5.6) still holds at 10^{16} GeV.

In this scenario, even though the RG evolution requirement is stronger than for scenario A, the softly broken $\mathbb{Z}_2$ symmetry $m_{12}^2 \neq 0$ allows large masses for the pseudoscalar (see Eq. (5.20)). Hence we find models with a BSM mass spectrum up to the upper bound of our scan range 1200 GeV. It is likely that there are viable models with Higgs masses beyond 1200 GeV.

The influence of $\tan\beta$ on the allowed masses for H at the electroweak scale is apparent in Fig. 11 where it is seen that the larger $\tan\beta$ the heavier H must be. This exclusion of light H bosons for large values of $\tan\beta$ is a consequence of the experimental constraints and can be understood from the Higgs couplings to bottom quarks which in type II (and type Y) 2HDMs is multiplied by a factor of [26]

$$H b\bar{b} \;:\; \frac{\cos\alpha}{\cos\beta}. \tag{5.30}$$

Thus when $\tan\beta$ is large, the coupling of H to the bottom quark is enhanced and hence the production cross section for H grows. In that case, H has to be heavy $m_H \gtrsim 700\,\text{GeV}$ otherwise it would have been detected.

In Fig. 12 it can be seen that the experimental constraints favour very small values of $c_{\beta-\alpha}$. Moreover the larger $\tan\beta$ the smaller $c_{\beta-\alpha}$ must be. Again this corresponds to models where the heavier scalar H doesn't couple to the weak bosons. Notice that there are no points that flow towards $c_{\beta-\alpha} \approx 1$ as in scenario A. One can also see that the value of $\tan\beta$ determines how much $c_{\beta-\alpha}$ can grow during RG evolution. Whereas for $\tan\beta = 25$ $c_{\beta-\alpha}$ remains very small, for $\tan\beta = 5$ it can grow as large as ~ 0.4. Even then $c^2_{\beta-\alpha}$ is still quite small. Therefore in this scenario it is still true at Λ_{FN} that the weak bosons mostly couple to the lighter scalar h.

Thus we find that the assumption that the physics at the electroweak scale is described by a 2HDM with a softly broken $\mathbb{Z}_2$ symmetry which is the low energy limit of a theory defined at $\Lambda_{FN} = 10^{16}\,\text{GeV}$ constrains the parameters of the theory at the electroweak scale. In particular, because the quartic couplings must be small, the RG flow is limited and correlations between the parameters of the models are approximately preserved during evolution. Hence in this scenario, our assumptions lead to models at $\Lambda_{FN} = 10^{16}\,\text{GeV}$ with mass degenerate BSM Higgs bosons. Moreover, in these models the heavier neutral scalar H remains weakly coupled to vector bosons.

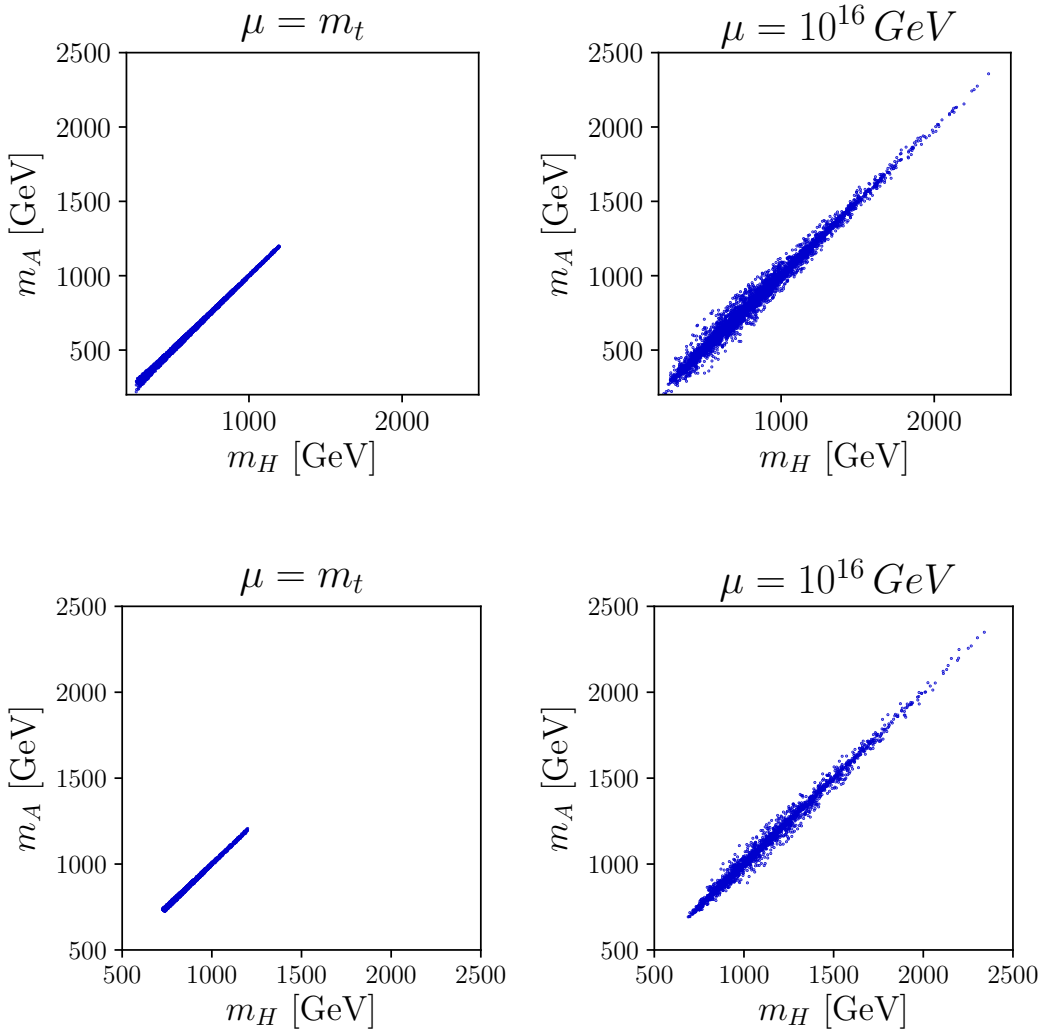

Figure 11: Top-left: $m_H - m_A$ plane of the region of well behaved models with $\tan\beta = 5$ consistent with experiments at the top mass scale m_t. Top-right: same region evolved to $\mu = 10^{16}\,\text{GeV}$. Bottom-left: $m_H - m_A$ plane of the region of well behaved models with $\tan\beta = 25$ consistent with experiments at the top mass scale m_t. Bottom-right: same region evolved to $\mu = 10^{16}\,\text{GeV}$.

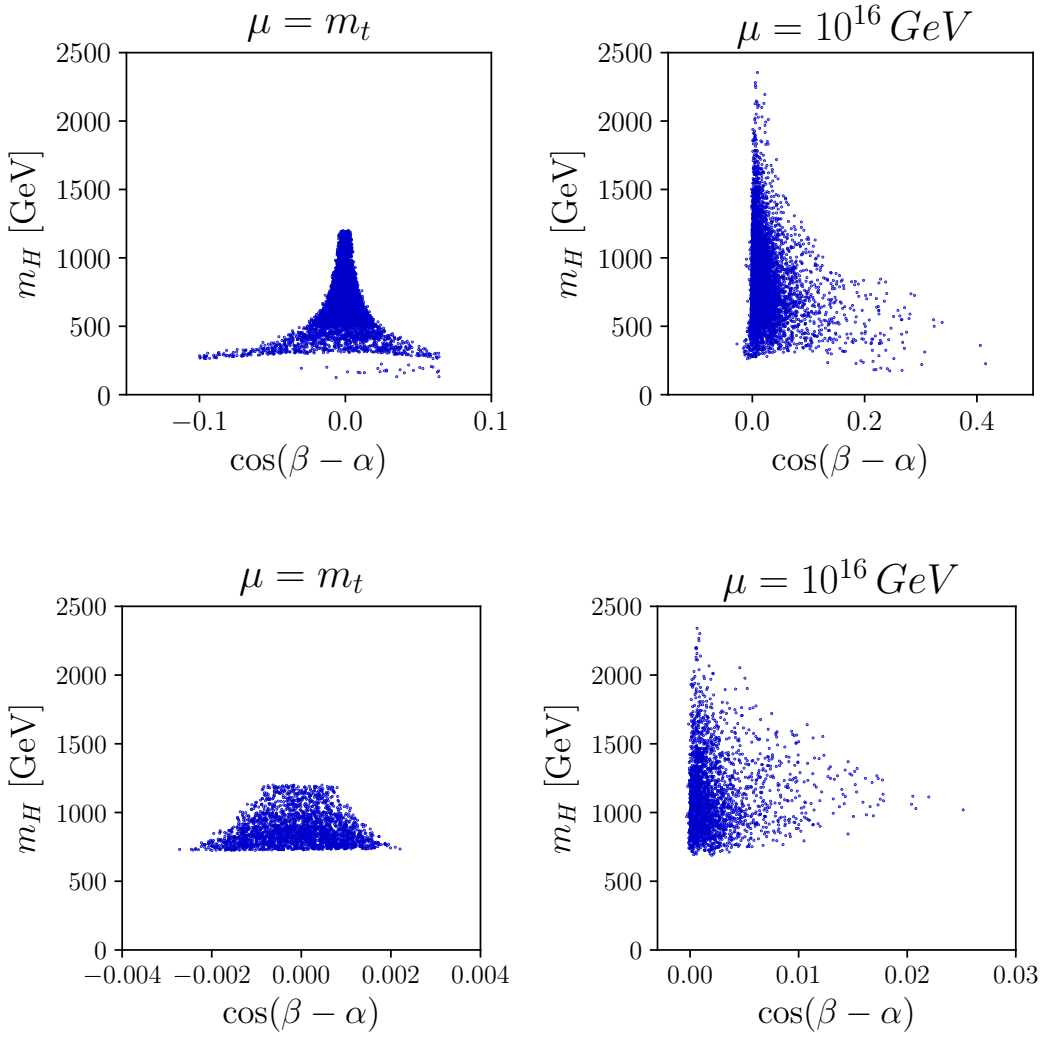

Figure 12: Top-left: $c_{\beta-\alpha} - m_H$ plane of the region of well behaved models with $\tan\beta = 5$ consistent with experiments at the top mass scale m_t. Top-right: same region evolved to $\mu = 10^{16}\,\text{GeV}$. Bottom-left: $c_{\beta-\alpha} - m_H$ plane of the region of well behaved models with $\tan\beta = 25$ consistent with experiments at the top mass scale m_t. Bottom-right: same region evolved to $\mu = 10^{16}\,\text{GeV}$.

6 Summary and Conclusions

In this thesis we have considered a 2HDM with a gauged Froggatt-Nielsen mechanism as an extension of the SM. These models can remove the hierarchy in the flavour parameters and inherit the rich phenomenology of 2HDMs. We assumed that such a model is the low-energy limit of a theory defined at the Froggatt-Nielsen scale Λ_{FN}. In order to constrain the 2HDM parameter space we started by using RG evolution and requiring stability, tree-level unitarity and perturbativity up to Λ_{FN}. To further constrain the 2HDM parameters, experimental constraints from Higgs searches were applied. We then attempted to build models in two scenarios: (A) the FN scale is low $\Lambda_{FN} = 10^5\,\text{GeV}$ and the $\mathbb{Z}_2$ symmetry is exact; (B) the FN scale is very high $\Lambda_{FN} = 10^{16}\,\text{GeV}$ and the $\mathbb{Z}_2$ symmetry is softly broken.

In scenario A we found that, because of the exact $\mathbb{Z}_2$ symmetry, the assumption that models can be evolved up to $10^5\,\text{GeV}$ requires $\tan\beta = \frac{v_2}{v_1} \approx 1$. In this scenario, it was found that RG evolution favours light BSM scalars. We could only find anomaly free sets of flavon charges reproducing realistic quark masses and mixing for type II models. Therefore viable models in scenario A are type II 2HDMs with $\tan\beta \approx 1$. Using RG evolution we were able to connect the electroweak scale to Λ_{FN}. Doing so we found that, at $\Lambda_{FN} = 10^5\,\text{GeV}$, the BSM Higgs bosons remain light and that in many models the lighter Higgs neutral scalar h decouples from the weak bosons.

In scenario B, where the FN scale is pushed to $10^{16}\,\text{GeV}$, we could find models which can be evolved up to Λ_{FN} for $\tan\beta = 1.1, 5, 25$. We found that the larger $\tan\beta$, the more constraining the RG evolution requirement. However it appears that models with $\tan\beta = 1.1$ require fine tuning between their parameters to be evolved up to $10^{16}\,\text{GeV}$ as we could only find a handful of points using uniform scans. As opposed to scenario A, the RG evolution requirement allowed for large BSM Higgs masses (up to at least $1200\,\text{GeV}$). In general, we found that models are constrained to have either very small $c_{\beta-\alpha}$ or $m_H \approx m_h$. Moreover in this scenario the BSM Higgs bosons are degenerate in mass i.e. $m_H \approx m_A \approx m_{H^\pm}$. We could find anomaly free sets of flavon charges for type II 2HDMs with $\tan\beta = 5$ and 25. Therefore viable models in scenario B are type II 2HDMs with $\tan\beta = 5, 25$. Because the RG evolution requirement is much stronger in this scenario, the quartic couplings are very small and the RG flow is limited. We found that during RG evolution the BSM Higgs masses increase and correlations between parameters observed at the electroweak scale are preserved. In particular, in this scenario no models exhibited decoupling of the lighter Higgs neutral scalar from the vector bosons at Λ_{FN}.

The models built in this work could be made more realistic. One could for instance include a mechanism to generate neutrino masses. Then one would have to reproduce the observed lepton mixing. The PMNS matrix can be included in the FN framework in the same way as the CKM. Accounting for lepton mixing in this way would simply introduce additional constraints on the flavon charges. Another idea to further constrain the flavon charges is to enforce cancellation of the $U(1)' \times U(1)' \times U(1)'$ and gravity $\times$ gravity $\times\, U(1)'$ anomalies. When these anomaly cancellation conditions are included, the Gröbner bases can contain higher order polynomials and hence the charges do not define a plane but a

more general algebraic curve.

Finally, one could make specific assumptions about the high energy theory and implement them in the RG evolution analysis by using different boundary conditions for the RG equations, for instance matching the 2HDM with a high energy theory such as the MSSM.

Acknowledgments

I would like to thank my supervisor, Johan Rathsman, for his continuous guidance and support throughout this project. I enjoyed our collaboration a great deal. Moreover, I am grateful to Joel Oredsson for his invaluable help with the programming aspects of this project and to Felix Tellander for helpful discussions on renormalization and algebraic geometry as well as for reviewing this thesis.

A 1-loop Correction to 2-2 Scattering in ϕ^4-theory

We want to calculate

$$i\mathcal{M}^{(\text{1-loop})} =$$ 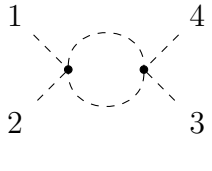

$$+$$ 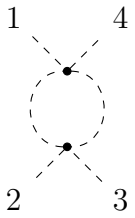

$$+ (3 \leftrightarrow 4)$$

Since we are looking to extract the UV divergence of this scattering amplitude we can work in the regime where $p_i << k$ and take all external momenta to 0. In that case

$$i\mathcal{M}^{(\text{1-loop})} = \frac{3}{2}(-i\lambda)^2 \int \frac{d^4k}{(2\pi)^4} \frac{i^2}{[k^2 - m^2 + i\varepsilon]^2} \equiv \frac{3\lambda^2}{2} V(0)$$

$$V(0) = \int \frac{d^4k}{(2\pi)^4} \frac{1}{[k^2 - m^2 + i\varepsilon]^2} = i \int \frac{d^4k_E}{(2\pi)^4} \frac{1}{[k_E^2 + m^2]^2}$$

where in the last step we have done a Wick rotation $k^0 \to ik^0$ so that $k^2 \to -k_E^2 = -(k_0^2 + k_1^2 + k_2^2 + k_3^2)$. $V(0) \sim \int \frac{d^4k_E}{k_E^4}$ diverges logarithmically. The divergence is extracted using dimensional regularization.

$$V_d(0) = \frac{i}{(2\pi)^4} \int d\Omega_d \int_0^\infty \frac{dk_E k_E^{d-1} \mu^{4-d}}{[k_E^2 + m^2]^2} = \frac{i}{(2\pi)^4} \frac{2\pi^{\frac{d}{2}}}{\Gamma(\frac{d}{2})} \int_0^\infty \frac{dk_E k_E^{d-1} \mu^{4-d}}{[k_E^2 + m^2]^2}$$

$$\Big\{ y = k_E^2 \Big\}$$

$$= \frac{i}{(2\pi)^4} \frac{\pi^{\frac{d}{2}}}{\Gamma(\frac{d}{2})} \mu^{4-d} \int_0^\infty \frac{dy y^{\frac{d}{2}-1}}{[y + m^2]^2} \qquad \Big\{ z = \frac{m^2}{y + m^2} \Big\}$$

$$= \frac{i}{(2\pi)^4} \frac{\pi^{\frac{d}{2}}}{\Gamma(\frac{d}{2})} \frac{\mu^{4-d}}{m^{4-d}} \int_0^1 dz z^{1-\frac{d}{2}} (1-z)^{\frac{d}{2}-1} = i \frac{\pi^{\frac{d}{2}}}{\Gamma(\frac{d}{2})} \frac{\mu^{4-d}}{m^{4-d}} \frac{\Gamma(\frac{d}{2})\Gamma(\frac{d}{2} - 2)}{\Gamma(2)}$$

$$= \frac{i}{(2\pi)^4} \pi^{\frac{d}{2}} \frac{\mu^{4-d}}{m^{4-d}} \Gamma\Big(\frac{d}{2} - 2\Big)$$

where μ is an energy scale introduced to keep $V(0)$ dimensionless and we have used the identity $\int_0^1 dz z^{\alpha-1}(1-z)^{\beta-1} = \frac{\Gamma(\alpha)\Gamma(\beta)}{\Gamma(\alpha+\beta)}$. The original integral converges in $d < 4$, so we let $d = 4 - \varepsilon$ and find

$$V_{4-\varepsilon}(0) = \frac{i}{16\pi^2} \Big(\frac{\mu}{m}\Big)^\varepsilon \Gamma\Big(\frac{\varepsilon}{2}\Big) = \frac{i}{8\pi^2} \frac{1}{\varepsilon} + \frac{i}{8\pi^2} \ln \frac{\mu}{m} + \text{finite terms}$$

where we have used $\Big(\frac{\mu}{m}\Big)^\varepsilon = 1 + \varepsilon \ln \frac{\mu}{m} + \mathcal{O}(\varepsilon^2)$ and the Laurent series of Γ around 0, $\Gamma(z) \approx \frac{1}{z}$. Thus our final result is

$$i\mathcal{M}^{(\text{1-loop})} = \frac{3\lambda^2}{2} V(0) = i \frac{3\lambda^2}{16\pi^2} \Big(\frac{1}{\varepsilon} + \ln \frac{\mu}{m} \Big).$$

B Anomaly-Free Sets of Charges in Scenario A

Type II, $\tan\beta = 1.1$

For this model we find the following Gröbner basis in `Sage`.

$$G = \Big\langle Q_1 + d_3 - \chi_2 + \frac{7}{3},\ u_1 - d_3 + 2\chi_2 - \frac{28}{3},\ d_1 - d_3 - 1,\ L_1 - \frac{9}{4}d_3 + \frac{1}{4}e_3 + 2\chi_2 - \frac{43}{6},$$
$$e_1 + \frac{9}{4}d_3 - \frac{1}{4}e_3 - 3\chi_2 + \frac{15}{2},\ Q_2 + d_3 - \chi_2 + \frac{10}{3},\ u_2 - d_3 + 2\chi_2 - \frac{19}{3},\ d_2 - d_3,$$
$$L_2 - \frac{27}{4}d_3 - \frac{5}{4}e_3 + 8\chi_2 - \frac{187}{6},\ e_2 + \frac{27}{4}d_3 + \frac{5}{4}e_3 - 9\chi_2 + \frac{71}{2},\ Q_3 + d_3 - \chi_2 + \frac{16}{3},$$
$$u_3 - d_3 + 2\chi_2 - \frac{16}{3},\ L_3 + e_3 - \chi_2 + \frac{16}{3},\ \chi_1 - \chi_2 + \frac{25}{3}\Big\rangle$$

The solutions can be parametrized by χ_2, d_3 and e_3

$$Q_1 = \chi_2 - d_3 - \frac{7}{3} \qquad Q_2 = \chi_2 - d_3 - \frac{10}{3} \qquad Q_3 = \chi_2 - d_3 - \frac{16}{3}$$
$$u_1 = -2\chi_2 + d_3 + \frac{28}{3} \qquad u_2 = -2\chi_2 + d_3 + \frac{19}{3} \qquad u_3 = -2\chi_2 + d_3 + \frac{16}{3}$$
$$d_1 = d_3 + 1 \qquad d_2 = d_3$$
$$L_1 = -2\chi_2 + \frac{9}{4}d_3 - \frac{1}{4}e_3 + \frac{43}{6} \qquad L_2 = -8\chi_2 + \frac{27}{4}d_3 + \frac{5}{4}e_3 + \frac{187}{6} \qquad L_3 = \chi_2 - e_3 - \frac{16}{3}$$
$$e_1 = 3\chi_2 - \frac{9}{4}d_3 + \frac{1}{4}e_3 - \frac{15}{2} \qquad e_2 = 9\chi_2 - \frac{27}{4}d_3 - \frac{5}{4}e_3 - \frac{71}{2}$$
$$\chi_1 = \chi_2 - \frac{25}{3}$$

Type X, $\tan\beta = 1.1$

For this model we find the following Gröbner basis in `Sage`.

$$G = \Big\langle Q_1 + d_3 - \chi_2 - 5,\ u_1 - d_3 + 2\chi_2 - 2,\ d_1 - d_3 + 12,\ L_1 - \frac{9}{4}d_3 + \frac{1}{4}e_3 + 2\chi_2 - \frac{1}{3},$$
$$e_1 + \frac{9}{4}d_3 - \frac{1}{4}e_3 - 3\chi_2 + \frac{2}{3},\ Q_2 + d_3 - \chi_2 - 4,\ u_2 - d_3 + 2\chi_2 + 1,\ d_2 - d_3 + 9,$$
$$L_2 - \frac{27}{4}d_3 - \frac{5}{4}e_3 + 8\chi_2 + 28,\ e_2 + \frac{27}{4}d_3 + \frac{5}{4}e_3 - 9\chi_2 - \frac{71}{3},\ Q_3 + d_3 - \chi_2 - 2,$$
$$u_3 - d_3 + 2\chi_2 + 2,\ L_3 + e_3 - \chi_2 + \frac{16}{3},\ \chi_1 - \chi_2 + \frac{25}{3}\Big\rangle$$

The solutions can be parametrized by χ_2, d_3 and e_3

$$
\begin{array}{lll}
Q_1 = \chi_2 - d_3 + 5 & Q_2 = \chi_2 - d_3 + 4 & Q_3 = \chi_2 - d_3 + 2 \\
u_1 = -2\chi_2 + d_3 + 2 & u_2 = -2\chi_2 + d_3 - 1 & u_3 = -2\chi_2 + d_3 - 2 \\
d_1 = d_3 - 12 & d_2 = d_3 - 9 & \\
L_1 = -2\chi_2 + \frac{9}{4}d_3 - \frac{1}{4}e_3 + \frac{1}{3} & L_2 = -8\chi_2 + \frac{27}{4}d_3 + \frac{5}{4}e_3 - 28 & L_3 = \chi_2 - e_3 - \frac{16}{3} \\
e_1 = 3\chi_2 - \frac{9}{4}d_3 + \frac{1}{4}e_3 - \frac{2}{3} & e_2 = 9\chi_2 - \frac{27}{4}d_3 - \frac{5}{4}e_3 + \frac{71}{3} & \\
\chi_1 = \chi_2 - \frac{25}{3} & &
\end{array}
$$

Type Y, $\tan\beta = 1.1$

For this model we find the following Gröbner basis in `Sage`.

$$
\begin{aligned}
G = \Big\langle & Q_1 + d_3 - \chi_2 + \frac{7}{3},\ u_1 - d_3 + 2\chi_2 - \frac{28}{3},\ d_1 - d_3 - 1,\ L_1 + \frac{3}{2}d_3 + \frac{3}{2}e_3 - 3\chi_2 + \frac{22}{3}, \\
& e_1 - \frac{3}{2}d_3 - \frac{3}{2}e_3 + 2\chi_2 + \frac{2}{3},\ Q_2 + d_3 - \chi_2 + \frac{10}{3},\ u_2 - d_3 + 2\chi_2 - \frac{19}{3},\ d_2 - d_3, \\
& L_2 - \frac{21}{2}d_3 - \frac{5}{2}e_3 + 13\chi_2 - \frac{115}{3},\ e_2 + \frac{21}{2}d_3 + \frac{5}{2}e_3 - 14\chi_2 + \frac{127}{3},\ Q_3 + d_3 - \chi_2 + \frac{16}{3}, \\
& u_3 - d_3 + 2\chi_2 - \frac{16}{3},\ L_3 + e_3 - \chi_2 - 2,\ \chi_1 - \chi_2 + \frac{25}{3}\Big\rangle
\end{aligned}
$$

The solutions can be parametrized by χ_2, d_3 and e_3

$$
\begin{array}{lll}
Q_1 = \chi_2 - d_3 - \frac{7}{3} & Q_2 = \chi_2 - d_3 - \frac{10}{3} & Q_3 = \chi_2 - d_3 - \frac{16}{3} \\
u_1 = -2\chi_2 + d_3 + \frac{28}{3} & u_2 = -2\chi_2 + d_3 + \frac{19}{3} & u_3 = -2\chi_2 + d_3 + \frac{16}{3} \\
d_1 = d_3 + 1 & d_2 = d_3 & \\
L_1 = 3\chi_2 - \frac{3}{2}d_3 - \frac{3}{2}e_3 - \frac{22}{3} & L_2 = -13\chi_2 + \frac{21}{2}d_3 + \frac{5}{2}e_3 + \frac{115}{3} & L_3 = \chi_2 - e_3 + 2 \\
e_1 = 2\chi_2 + \frac{3}{2}d_3 + \frac{3}{2}e_3 - \frac{2}{3} & e_2 = 14\chi_2 - \frac{21}{2}d_3 - \frac{5}{2}e_3 - \frac{127}{3} & \\
\chi_1 = \chi_2 - \frac{25}{3} & &
\end{array}
$$

C Anomaly-Free Sets of Charges in Scenario B

Type II, $\tan\beta = 1.1$

For this model we find the following Gröbner basis in `Sage`.

$$G = \Big\langle Q_1 + d_3 - \chi_2 + 3,\ u_1 - d_3 + 2\chi_2 - 10,\ d_1 - d_3 - 1,\ L_1 - d_3 + \frac{2}{3}e_3 + \frac{1}{3}\chi_2 - \frac{2}{3},$$
$$e_1 + d_3 - \frac{2}{3}e_3 - \frac{4}{3}\chi_2 + \frac{5}{3},\ Q_2 + d_3 - \chi_2 + 4,\ u_2 - d_3 + 2\chi_2 - 8,\ d_2 - d_3 - 1,$$
$$L_2 - 8d_3 - \frac{5}{3}e_3 + \frac{29}{3}\chi_2 - \frac{133}{3},\ e_2 + 8d_3 + \frac{5}{3}e_3 - \frac{32}{3}\chi_2 + \frac{145}{3},\ Q_3 + d_3 - \chi_2 + 6,$$
$$u_3 - d_3 + 2\chi_2 - 6,\ L_3 + e_3 - \chi_2 + 6,\ \chi_1 - \chi_2 + 9\Big\rangle$$

The solutions can be parametrized by χ_2, d_3 and e_3

$$\begin{array}{lll}
Q_1 = \chi_2 - d_3 - 3 & Q_2 = \chi_2 - d_3 - 4 & Q_3 = \chi_2 - d_3 - 6 \\
u_1 = -2\chi_2 + d_3 + 10 & u_2 = -2\chi_2 + d_3 + 8 & u_3 = -2\chi_2 + d_3 + 6 \\
d_1 = d_3 + 1 & d_2 = d_3 + 1 & \\
L_1 = -\frac{1}{3}\chi_2 + d_3 - \frac{2}{3}e_3 + \frac{2}{3} & L_2 = -\frac{29}{3}\chi_2 + 8d_3 + \frac{5}{3}e_3 + \frac{133}{3} & L_3 = \chi_2 - e_3 - 6 \\
e_1 = \frac{4}{3}\chi_2 - d_3 + \frac{2}{3}e_3 - \frac{5}{3} & e_2 = \frac{32}{3}\chi_2 - 8d_3 - \frac{5}{3}e_3 - \frac{145}{3} & \\
\chi_1 = \chi_2 - 9 & &
\end{array}$$

Type II, $\tan\beta = 5$

For this model we find the following Gröbner basis in `Sage`.

$$G = \Big\langle Q_1 + d_3 - \chi_2 + \frac{11}{3},\ u_1 - d_3 + 2\chi_2 - \frac{35}{3},\ d_1 - d_3 - 1,\ L_1 - d_3 + \frac{2}{3}e_3 + \frac{1}{3}\chi_2 - \frac{2}{3},$$
$$e_1 + d_3 - \frac{2}{3}e_3 - \frac{4}{3}\chi_2 + \frac{7}{3},\ Q_2 + d_3 - \chi_2 + \frac{14}{3},\ u_2 - d_3 + 2\chi_2 - \frac{26}{3},\ d_2 - d_3 - 1,$$
$$L_2 - 8d_3 - \frac{5}{3}e_3 + \frac{29}{3}\chi_2 - 51,\ e_2 + 8d_3 + \frac{5}{3}e_3 - \frac{32}{3}\chi_2 + \frac{167}{3},\ Q_3 + d_3 - \chi_2 + \frac{20}{3},$$
$$u_3 - d_3 + 2\chi_2 - \frac{23}{3},\ L_3 + e_3 - \chi_2 + \frac{20}{3},\ \chi_1 - \chi_2 + \frac{26}{3}\Big\rangle$$

The solutions can be parametrized by χ_2, d_3 and e_3

$$
\begin{aligned}
Q_1 &= \chi_2 - d_3 - \frac{11}{3} & Q_2 &= \chi_2 - d_3 - \frac{14}{3} & Q_3 &= \chi_2 - d_3 - \frac{20}{3} \\
u_1 &= -2\chi_2 + d_3 + \frac{35}{3} & u_2 &= -2\chi_2 + d_3 + \frac{26}{3} & u_3 &= -2\chi_2 + d_3 + \frac{23}{3} \\
d_1 &= d_3 + 1 & d_2 &= d_3 + 1 & & \\
L_1 &= -\frac{1}{3}\chi_2 + d_3 - \frac{2}{3}e_3 + \frac{2}{3} & L_2 &= -\frac{29}{3}\chi_2 + 8d_3 + \frac{5}{3}e_3 + 51 & L_3 &= \chi_2 - e_3 - \frac{20}{3} \\
e_1 &= \frac{4}{3}\chi_2 - d_3 + \frac{2}{3}e_3 - \frac{7}{3} & e_2 &= \frac{32}{3}\chi_2 - 8d_3 - \frac{5}{3}e_3 - \frac{167}{3} & & \\
\chi_1 &= \chi_2 - \frac{26}{3} & & & &
\end{aligned}
$$

Type II, $\tan\beta = 25$

For this model we find the following Gröbner basis in `Sage`.

$$
\begin{aligned}
G = \Big\langle & Q_1 + d_3 - \chi_2 + \frac{11}{3},\ u_1 - d_3 + 2\chi_2 - \frac{35}{3},\ d_1 - d_3 - 1,\ L_1 - d_3 + \frac{2}{3}e_3 + \frac{1}{3}\chi_2 - \frac{2}{3}, \\
& e_1 + d_3 - \frac{2}{3}e_3 - \frac{4}{3}\chi_2 + \frac{7}{3},\ Q_2 + d_3 - \chi_2 + \frac{14}{3},\ u_2 - d_3 + 2\chi_2 - \frac{26}{3},\ d_2 - d_3 - 1, \\
& L_2 - 8d_3 - \frac{5}{3}e_3 + \frac{29}{3}\chi_2 - 51,\ e_2 + 8d_3 + \frac{5}{3}e_3 - \frac{32}{3}\chi_2 + \frac{167}{3},\ Q_3 + d_3 - \chi_2 + \frac{20}{3}, \\
& u_3 - d_3 + 2\chi_2 - \frac{23}{3},\ L_3 + e_3 - \chi_2 + \frac{20}{3},\ \chi_1 - \chi_2 + \frac{23}{3}\Big\rangle
\end{aligned}
$$

The solutions can be parametrized by χ_2, d_3 and e_3

$$
\begin{aligned}
Q_1 &= \chi_2 - d_3 - \frac{11}{3} & Q_2 &= \chi_2 - d_3 - \frac{14}{3} & Q_3 &= \chi_2 - d_3 - \frac{20}{3} \\
u_1 &= -2\chi_2 + d_3 + \frac{35}{3} & u_2 &= -2\chi_2 + d_3 + \frac{26}{3} & u_3 &= -2\chi_2 + d_3 + \frac{23}{3} \\
d_1 &= d_3 + 1 & d_2 &= d_3 + 1 & & \\
L_1 &= -\frac{1}{3}\chi_2 + d_3 - \frac{2}{3}e_3 + \frac{2}{3} & L_2 &= -\frac{29}{3}\chi_2 + 8d_3 + \frac{5}{3}e_3 + 51 & L_3 &= \chi_2 - e_3 - \frac{20}{3} \\
e_1 &= \frac{4}{3}\chi_2 - d_3 + \frac{2}{3}e_3 - \frac{7}{3} & e_2 &= \frac{32}{3}\chi_2 - 8d_3 - \frac{5}{3}e_3 - \frac{167}{3} & & \\
\chi_1 &= \chi_2 - \frac{23}{3} & & & &
\end{aligned}
$$

Type X, $\tan\beta = 5$

For this model we find the following Gröbner basis in `Sage`.

$$G = \Big\langle Q_1 + d_3 - \chi_2 - 6,\ u_1 - d_3 + 2\chi_2 + 14,\ d_1 - d_3 - 1,\ L_1 - d_3 + \frac{2}{3}e_3 + \frac{1}{3}\chi_2 + \frac{61}{3},$$
$$e_1 + d_3 - \frac{2}{3}e_3 - \frac{4}{3}\chi_2 - \frac{73}{3},\ Q_2 + d_3 - \chi_2 - 5,\ u_2 - d_3 + 2\chi_2 + 1,\ d_2 - d_3 + 11,$$
$$L_2 - 8d_3 - \frac{5}{3}e_3 + \frac{29}{3}\chi_2 + \frac{62}{3},\ e_2 + 8d_3 + \frac{5}{3}e_3 - \frac{32}{3}\chi_2 - \frac{65}{3},\ Q_3 + d_3 - \chi_2 - 3,$$
$$u_3 - d_3 + 2\chi_2 + 3,\ L_3 + e_3 - \chi_2 + 1,\ \chi_1 - \chi_2 + 3\Big\rangle$$

The solutions can be parametrized by χ_2, d_3 and e_3

$$\begin{array}{lll}
Q_1 = \chi_2 - d_3 + 6 & Q_2 = \chi_2 - d_3 + 5 & Q_3 = \chi_2 - d_3 + 3 \\
u_1 = -2\chi_2 + d_3 - 14 & u_2 = -2\chi_2 + d_3 - 1 & u_3 = -2\chi_2 + d_3 - 3 \\
d_1 = d_3 + 1 & d_2 = d_3 + 11 & \\
L_1 = -\frac{1}{3}\chi_2 + d_3 - \frac{2}{3}e_3 - \frac{61}{3} & L_2 = -\frac{29}{3}\chi_2 + 8d_3 + \frac{5}{3}e_3 - \frac{62}{3} & L_3 = \chi_2 - e_3 - 1 \\
e_1 = \frac{4}{3}\chi_2 - d_3 + \frac{2}{3}e_3 + \frac{73}{3} & e_2 = \frac{32}{3}\chi_2 - 8d_3 - \frac{5}{3}e_3 + \frac{65}{3} & \\
\chi_1 = \chi_2 - 3 & &
\end{array}$$

Type X, $\tan\beta = 25$

For this model we find the following Gröbner basis in `Sage`.

$$G = \Big\langle Q_1 + d_3 - \chi_2 - 6,\ u_1 - d_3 + 2\chi_2 + 14,\ d_1 - d_3 - 1,\ L_1 - d_3 + \frac{2}{3}e_3 + \frac{1}{3}\chi_2 + \frac{61}{3},$$
$$e_1 + d_3 - \frac{2}{3}e_3 - \frac{4}{3}\chi_2 - \frac{73}{3},\ Q_2 + d_3 - \chi_2 - 5,\ u_2 - d_3 + 2\chi_2 + 1,\ d_2 - d_3 + 11,$$
$$L_2 - 8d_3 - \frac{5}{3}e_3 + \frac{29}{3}\chi_2 + \frac{62}{3},\ e_2 + 8d_3 + \frac{5}{3}e_3 - \frac{32}{3}\chi_2 - \frac{65}{3},\ Q_3 + d_3 - \chi_2,$$
$$u_3 - d_3 + 2\chi_2 + 3,\ L_3 + e_3 - \chi_2 + 1,\ \chi_1 - \chi_2 + 2\Big\rangle$$

The solutions can be parametrized by χ_2, d_3 and e_3

$$\begin{array}{lll}
Q_1 = \chi_2 - d_3 + 6 & Q_2 = \chi_2 - d_3 + 5 & Q_3 = \chi_2 - d_3 + 3 \\
u_1 = -2\chi_2 + d_3 - 14 & u_2 = -2\chi_2 + d_3 - 1 & u_3 = -2\chi_2 + d_3 - 3 \\
d_1 = d_3 + 1 & d_2 = d_3 + 11 & \\
L_1 = -\frac{1}{3}\chi_2 + d_3 - \frac{2}{3}e_3 - \frac{61}{3} & L_2 = -\frac{29}{3}\chi_2 + 8d_3 + \frac{5}{3}e_3 - \frac{62}{3} & L_3 = \chi_2 - e_3 - 1 \\
e_1 = \frac{4}{3}\chi_2 - d_3 + \frac{2}{3}e_3 + \frac{73}{3} & e_2 = \frac{32}{3}\chi_2 - 8d_3 - \frac{5}{3}e_3 + \frac{65}{3} & \\
\chi_1 = \chi_2 - 2 & &
\end{array}$$

Type Y, $\tan\beta = 1.1$

For this model we find the following Gröbner basis in `Sage`.

$$G = \Big\langle Q_1 + d_3 - \chi_2 - \frac{20}{3},\ u_1 - d_3 + 2\chi_2 - \frac{44}{3},\ d_1 - d_3 + 7,\ L_1 - \frac{51}{11}d_3 - \frac{6}{11}e_3 + \frac{57}{11}\chi_2 + \frac{983}{33},$$
$$e_1 + \frac{51}{11}d_3 + \frac{6}{11}e_3 - \frac{68}{11}\chi_2 - \frac{1214}{33},\ Q_2 + d_3 - \chi_2 - \frac{17}{3},\ u_2 - d_3 + 2\chi_2 + \frac{8}{3},\ d_2 - d_3 + 4,$$
$$L_2 - \frac{48}{11}d_3 - \frac{5}{11}e_3 + \frac{53}{11}\chi_2 + \frac{667}{33},\ e_2 + \frac{48}{11}d_3 + \frac{5}{11}e_3 - \frac{64}{11}\chi_2 - \frac{535}{33},\ Q_3 + d_3 - \chi_2 - \frac{11}{3},$$
$$u_3 - d_3 + 2\chi_2 + \frac{11}{3},\ L_3 + e_3 - \chi_2 - 2,\ \chi_1 - \chi_2 - \frac{20}{3}\Big\rangle$$

The solutions can be parametrized by χ_2, d_3 and e_3

$$Q_1 = \chi_2 - d_3 + \frac{20}{3} \qquad Q_2 = \chi_2 - d_3 + \frac{17}{3} \qquad Q_3 = \chi_2 - d_3 + \frac{11}{3}$$
$$u_1 = -2\chi_2 + d_3 + \frac{44}{3} \qquad u_2 = -2\chi_2 + d_3 - \frac{8}{3} \qquad u_3 = -2\chi_2 + d_3 - \frac{11}{3}$$
$$d_1 = d_3 + 1 \qquad d_2 = d_3 + 1$$
$$L_1 = -\frac{57}{11}\chi_2 + \frac{51}{11}d_3 + \frac{6}{11}e_3 - \frac{989}{33} \qquad L_2 = -\frac{53}{11}\chi_2 + \frac{48}{11}d_3 + \frac{5}{11}e_3 + \frac{667}{33} \qquad L_3 = \chi_2 - e_3 + 2$$
$$e_1 = \frac{68}{11}\chi_2 - \frac{51}{11}d_3 - \frac{6}{11}e_3 + \frac{1214}{33} \qquad e_2 = \frac{64}{11}\chi_2 - \frac{48}{11}d_3 - \frac{5}{11}e_3 + \frac{535}{33}$$
$$\chi_1 = \chi_2 + \frac{20}{3}$$

References

[1] Y. Grossman and P. Tanedo, *Just a Taste: Lectures on Flavor Physics*, in *Proceedings TASI 2016*, pp. 109–295, 2018, 1711.03624, DOI.

[2] ATLAS collaboration, *Observation of a new particle in the search for the Standard Model Higgs boson with the ATLAS detector at the LHC*, *Phys. Lett.* **B716** (2012) 1 [1207.7214].

[3] H. Georgi and S. L. Glashow, *Unity of All Elementary Particle Forces*, *Phys. Rev. Lett.* **32** (1974) 438.

[4] D. Das and P. B. Pal, *S_3 flavored left-right symmetric model of quarks*, *Phys. Rev.* **D98** (2018) 115001 [1808.02297].

[5] C. Froggatt and H. Nielsen, *Hierarchy of quark masses, cabibbo angles and cp violation*, *Nuclear Physics B* **147** (1979) 277 .

[6] G. C. Branco, P. M. Ferreira, L. Lavoura, M. N. Rebelo, M. Sher and J. P. Silva, *Theory and phenomenology of two-Higgs-doublet models*, *Phys. Rept.* **516** (2012) 1 [1106.0034].

[7] S. L. Glashow and S. Weinberg, *Natural Conservation Laws for Neutral Currents*, *Phys. Rev.* **D15** (1977) 1958.

[8] I. Ginzburg, *Different vacua in 2HDM*, *eConf* **C0705302** (2007) HIG02 [0704.3664].

[9] H. E. Haber and O. Stål, *New LHC benchmarks for the $\mathcal{CP}$ -conserving two-Higgs-doublet model*, *Eur. Phys. J.* **C75** (2015) 491 [1507.04281].

[10] G. Strang, *Linear algebra and its applications*. Thomson Brooks/Cole, 2006.

[11] Particle Data Group collaboration, *Review of Particle Physics*, *Phys. Rev.* **D98** (2018) 030001.

[12] J. Rathsman and F. Tellander, *Anomaly-free Model Building with Algebraic Geometry*, 1902.08529.

[13] L. Wolfenstein, *Parametrization of the Kobayashi-Maskawa Matrix*, *Phys. Rev. Lett.* **51** (1983) 1945.

[14] A. Bilal, *Lectures on Anomalies*, 0802.0634.

[15] S. Weinberg, *The quantum theory of fields. Vol. 2: Modern applications*. Cambridge University Press, 2013.

[16] The Sage Developers, *SageMath, the Sage Mathematics Software System (Version 8.4)*, 2018.

[17] D. A. Cox, J. Little and D. O'Shea, *Ideals, Varieties, and Algorithms: An Introduction to Computational Algebraic Geometry and Commutative Algebra*. Springer-Verlag, Berlin, Heidelberg, 2007.

[18] M. E. Peskin and D. V. Schroeder, *An Introduction to quantum field theory*. Addison-Wesley, Reading, USA, 1995.

[19] J. Oredsson and J. Rathsman, *$\mathbb{Z}_2$ breaking effects in 2-loop RG evolution of 2HDM*, *JHEP* **02** (2019) 152 [1810.02588].

[20] J. Oredsson, *2 Higgs Doublet Model Evolver - Manual*, 1811.08215.

[21] A. W. El Kaffas, W. Khater, O. M. Ogreid and P. Osland, *Consistency of the two Higgs doublet model and CP violation in top production at the LHC*, *Nucl. Phys.* **B775** (2007) 45 [hep-ph/0605142].

[22] I. F. Ginzburg and I. P. Ivanov, *Tree-level unitarity constraints in the most general 2HDM*, *Phys. Rev.* **D72** (2005) 115010 [hep-ph/0508020].

[23] B. Grinstein, C. W. Murphy and P. Uttayarat, *One-loop corrections to the perturbative unitarity bounds in the CP-conserving two-Higgs doublet model with a softly broken $\mathbb{Z}_2$ symmetry*, *JHEP* **06** (2016) 070 [1512.04567].

[24] Z.-z. Xing, H. Zhang and S. Zhou, *Updated Values of Running Quark and Lepton Masses*, *Phys. Rev.* **D77** (2008) 113016 [0712.1419].

[25] D. Buttazzo, G. Degrassi, P. P. Giardino, G. F. Giudice, F. Sala, A. Salvio et al., *Investigating the near-criticality of the Higgs boson*, *JHEP* **12** (2013) 089 [1307.3536].

[26] J. F. Gunion, S. Dawson, H. E. Haber and G. L. Kane, *The Higgs Hunter's Guide*, vol. 80. Brookhaven Nat. Lab., Upton, NY, 1989.

[27] P. Bechtle, O. Brein, S. Heinemeyer, G. Weiglein and K. E. Williams, *HiggsBounds: Confronting Arbitrary Higgs Sectors with Exclusion Bounds from LEP and the Tevatron*, *Comput. Phys. Commun.* **181** (2010) 138 [0811.4169].

[28] P. Bechtle, S. Heinemeyer, O. Stål, T. Stefaniak and G. Weiglein, *HiggsSignals: Confronting arbitrary Higgs sectors with measurements at the Tevatron and the LHC*, *Eur. Phys. J.* **C74** (2014) 2711 [1305.1933].

[29] D. Eriksson, J. Rathsman and O. Stål, *2HDMC: Two-Higgs-doublet model calculator*, *Comput. Phys. Commun.* **181** (2010) 833.

[30] H. Georgi and C. Jarlskog, *A New Lepton - Quark Mass Relation in a Unified Theory*, *Phys. Lett.* **86B** (1979) 297.